Quadrature Amplitude Modulated Codes with Low Peak-to-Mean Envelope Power Ratio for Orthogonal Frequency Division Multiplexing Applications

by

Chan Vee Chong

B.S.E., Electrical Engineering
Princeton University, 1999

Submitted to the Department of Electrical Engineering and Computer Science
in partial fulfillment of the requirements for the degree of

Master of Science in Electrical Engineering and Computer Science

at the

MASSACHUSETTS INSTITUTE OF TECHNOLOGY

May 2001

Author .....
Department of Electrical Engineering and Computer Science
May 21, 2001

Certified by .....
Vahid Tarokh
Associate Professor
Thesis Supervisor

Accepted by .....
Arthur C. Smith
Chairman, Department Committee on Graduate Students

Quadrature Amplitude Modulated Codes with Low Peak-to-Mean Envelope Power Ratio for Orthogonal Frequency Division Multiplexing Applications

by

Chan Vee Chong

Submitted to the Department of Electrical Engineering and Computer Science
on May 21, 2001, in partial fulfillment of the
requirements for the degree of
Master of Science in Electrical Engineering and Computer Science

Abstract

Orthogonal Frequency Division Multiplexing (OFDM) has been adopted as the modulation technique for many of the next generation wireless broadband multimedia communications systems, for example, Digital Audio Broadcasting (DAB), terrestrial Digital Video Broadcasting (DVB), and the wireless local area network (LAN) standards HIPERLAN/2, and IEEE 802.11a.

One problem inherent in plain vanilla OFDM is that its signal envelope fluctuates greatly with very high power peaks, necessitating the use of inefficient and complex linear power amplifiers. Solutions to the high peak-to-mean envelope power ratio (PMEPR) problem include signal processing techniques such as clipping, peak windowing, and peak cancellation, as well as coding techniques, i.e. using codes to ensure that only those OFDM signals with low PMEPR are transmitted. It is well known that using codewords generated by mapping binary Golay complementary sequences into BPSK yields OFDM signals with low PMEPR.

Frank, Sivaswamy, and others have extended the results of Golay from binary phase shift keying (BPSK) to other PSK constellations. Recently, Davis and Jedwab presented a code structure for these PSK complementary sequences using cosets of first-order Reed-Muller codes in second-order Reed-Muller codes. This yielded OFDM codes using PSK modulation which could be encoded and decoded using well-understood algorithms for Reed-Muller codes.

This thesis investigates the properties of *quadrature amplitude modulated (QAM)* OFDM signals with low PMEPR, focusing in particular on signals based on 4-QAM and 16-QAM constellations. We construct and prove new code structures for sequences in 4-QAM and 16-QAM that result OFDM signals with low PMEPR. Many practical implementations of OFDM use QAM constellations instead of PSK constellations. Thus the codes presented could be used to design pilot symbols for actual OFDM systems, as well as be employed in practical OFDM applications requiring both low PMEPR as well as low computational complexity.

Thesis Supervisor: Vahid Tarokh
Title: Associate Professor

Acknowledgments

First and foremost, I would like to thank my advisor, Prof. Vahid Tarokh, for all his help and advice, from proposing a myriad of possible thesis topics in the beginning, to advising on the writing of this thesis at the end. I will always remember his infectious enthusiasm, high energy level, and "open-door policy" (he always spared me time to discuss about my research every single time I dropped by his office without an appointment). This thesis would not have been possible without him.

I would also like to thank my family for their constant encouragement and support, and my friends at MIT for keeping me sane and showing me that there is more to MIT than just classes and research.

My deepest heartfelt gratitude goes to these very special individuals—my best friend, Momo, for lifting up my spirits when I was down, and prodding me on when I stalled on my work; Deedee, for his understanding, patience, and listening ear; and Tracey, for being the inspiration and motivation that led to the most original parts of this thesis.

Contents

1 Introduction **13**

2 Orthogonal Frequency Division Multiplexing (OFDM) Basics **17**

2.1 Generation of Basic OFDM Signal Using the IFFT 17

2.2 Guard Time and Cyclic Extension 20

2.3 Windowing 22

2.4 OFDM Receiver Operation 23

3 The Peak-to-Mean Envelope Power Ratio (PMEPR) Problem **27**

3.1 Mathematical Definition 28

3.2 Distribution of the PMEPR 29

3.2.1 Distribution in Time 29

3.2.2 Distribution of PMEPR per OFDM Symbol 31

3.3 Solutions to the PMEPR Problem 33

3.3.1 Clipping and Peak Windowing 33

3.3.2 Peak Cancellation 33

3.3.3 Other Solutions 35

4 PMEPR Reducing Codes **39**

4.1 Golay Complementary Sequences 40

4.2 Golay Complementary Sequences and Reed-Muller Codes 42

4.2.1 Boolean Functions and Reed-Muller Codes 42

4.2.2 Theorem of Davis and Jedwab 43

5 Quadrature Amplitude Modulated (QAM) Codes with Low PMEPR **47**

5.1 Preliminaries 48

5.1.1 Constellations for Quadrature Amplitude Modulation 48
5.1.2 Notation and Definitions 48
5.2 Properties of Complementary QAM Sequences 49
5.2.1 Transforms that Preserve Complementarity 49
5.2.2 Length Extension of Complementary Sequences 52
5.3 Construction of 4-QAM Sequences with Low PMEPR 55
5.3.1 A Link Between BPSK and 4-QAM Constellations 55
5.3.2 Construction of 4-QAM Codes from BPSK Codes 57
5.3.3 Construction of Sequences with PMEPR ≤ 4 58
5.3.4 ML OFDM Decoding Algorithm for Constructed Code 58
5.4 Construction of Complementary 16-QAM Sequences from 4-QAM Sequences 61
5.5 16-QAM Complementary Sequences formed from one 4-QAM Complementary Pair 63
5.6 16-QAM Complementary Sequences formed from 4-QAM Complementary Sequences as described by Davis and Jedwab 64
5.6.1 Theorem 64
5.6.2 Proof 65
5.6.3 PMEPR Bounds for Constructed Complementary 16-QAM Sequences 76
5.6.4 Code Rates for Constructed Complementary 16-QAM Sequences . . 77
5.7 8-QAM Complementary Sequences 79

6 Conclusion **81**
6.1 Summary 81
6.2 Future Research Possibilities 81

List of Figures

2-1 Spectra of Individual Subcarriers 19
2-2 Effect of multipath with zero signal in the guard time 21
2-3 OFDM symbol with cyclic extension 21
2-4 Example of an OFDM signal in multipath channel 22
2-5 Raised cosine window for OFDM symbol 23
2-6 Block diagram of an OFDM transceiver 24

3-1 16-channel OFDM signal with worst case PMEPR 27
3-2 PMEPR distribution in time 30
3-3 PMEPR distribution without oversampling 31
3-4 PMEPR distribution with oversampling 32
3-5 Windowing an OFDM time signal 34
3-6 Frequency spectra of clipping vs. peak windowing 35
3-7 Frequency spectrum after peak windowing for various window lengths . . . 36
3-8 Peak cancellation: original signal envelope and cancellation signal envelope 36
3-9 Peak cancellation: original signal envelope and signal envelope after cancellation 37
3-10 Power spectral density after peak cancellation 37

5-1 4-QAM, 16-QAM, and 64-QAM signal constellations 48
5-2 4-QAM constellation as the 'sum' of two BPSK 56
5-3 Constructing 16-QAM symbols from two 4-QAM symbols 61
5-4 Subsets of 16-QAM constellation points used when $s_0 = 0, 1, 2, 3$ 69
5-5 Graphical representation of construction of 16-QAM symbols 77
5-6 8-QAM Signal Constellation 80

List of Tables

5.1 Values for the third factor $\xi^{i_s} + \xi^{-(i+u)_s}$ for cases $s(x_1, x_2, \cdots, x_m) = x_{\pi(m)}$, $2x_{\pi(m)}$, $3x_{\pi(m)}$, $\mathbf{1} + x_{\pi(m)}$, $\mathbf{1} + 3x_{\pi(m)}$ 70

5.2 Values for the third factor $\xi^{i_s} + \xi^{-(i+u)_s}$ for cases $s(x_1, x_2, \cdots, x_m) = x_{\pi(w)} + 3x_{\pi(w+1)}$, $2x_{\pi(w)} + 2x_{\pi(w+1)}$, $3x_{\pi(w)} + x_{\pi(w+1)}$, $\mathbf{1} + x_{\pi(w)} + x_{\pi(w+1)}$, $\mathbf{1} + 3x_{\pi(w)} + 3x_{\pi(w+1)}$ 75

5.3 PMEPR bounds for constructed 16-QAM sequences 78

5.4 No. of constructed 16-QAM sequences grouped according to PMEPR bound 79

5.5 Code rates of constructed 16-QAM sequences 79

Chapter 1

Introduction

The explosive growth in the use of the Internet has led directly to rapidly increasing demand for higher and higher data speeds over both wired and wireless links. In the pursuit of high data rates over untethered connections, we find that present modulation techniques for wireless communications using a single carrier, such as direct sequence spread spectrum (DSSS), only scale up to a certain point before the growth in receiver complexity outstrips our ability to implement the system in a cost-effective manner.

One of the major constraints in wireless communications that is limiting the scalability of single-carrier techniques is the multipath fading environment. A signal from a transmitter can take multiple paths to reach the receiver. Each signal travels over a different distance and suffers different levels of attenuation and phase shifts. So what the receiver receives is the sum of multiple copies of the transmitted signal with varying signal strength, spread in time and distorted by noise.

The spread in time, called the multipath delay spread, is primarily determined by the physical environment—the relative locations of the transmitter, the receiver, and objects that reflect the transmitted signal. It does not depend on the data rate of the transmitted signal. So as we push up the data rates on present single-carrier systems by having symbols and chips of shorter and shorter duration, we find the relative ratio of multipath delay spread to the symbol duration increasing to such levels that intersymbol interference (ISI) becomes significant. This means that signals arriving at the receiver after travelling along longer paths interfere with signals that were transmitted several symbols later but reach the receiver earlier having travelled through shorter paths. This multipath delay spread can be

exploited to our advantage by using equalizers and Rake receiver structures so that what was intersymbol interference before gives us valuable diversity gain.

However, as symbol durations become even shorter (while the multipath delay spread remains unchanged), the relative ratio of multipath delay spread to the symbol duration increases. As the complexity of the receiver structure required to achieve diversity gain increases exponentially with the number of chip durations over which it has to track the received signal, it has become practically unfeasible to continue using single carrier systems for the data rates that we desire in next generation wireless broadband multimedia communication systems. A rough approximation of the increase in receiver complexity is that for every order of magnitude the data rate increases, the complexity increases by about twice that order.

One of the most promising approaches to solving this problem is to use multiple carriers instead. This method lets us split a high data rate input into multiple parallel lower rate data streams, which are then transmitted simultaneously over different subcarrier frequencies. The lower data rate on each subcarrier allows us to use a longer symbol duration, hence alleviating the problems of intersymbol interference and receiver complexity.

Compared to the single-carrier spread spectrum systems, the multi-carrier approach shifts complexity in the system from the equalizer/Rake receiver to a Fourier transform computation. Due to the existence of Fast Fourier Transform algorithms requiring only $O(n \log n)$ operations for n sub-carriers, the complexity has been rendered much easier to manage, as compared to single-carrier systems.

There are various flavors of multi-carrier communications techniques, including Multi-Carrier Code Division Multiple Access (MC-CDMA), Multi-carrier Direct Sequence-CDMA and Multitone CDMA (MT-CDMA). For the purposes of this thesis, we will be focussing only on the basic multi-carrier technique, known as Orthogonal Frequency Division Multiplexing (OFDM). Chapter Two will describe the basics of OFDM.

As appealing as the idea of OFDM looks on paper, there are certain issues that need to be resolved before we can successfully realize an OFDM system. One of these issues concerns the fluctuating signal envelope with high power peaks that results from straightforward application of the OFDM concept. The extremely high peak envelope power to average power ratio necessitates the use of inefficient and complex linear power amplifiers. Chapter Three will describe this Peak-to-Mean Envelope Power Ratio (PMEPR) problem in detail

and present several solutions to the problem.

One category of solutions to the PMEPR problem uses coding techniques so that the signals produced at the transmitter are guaranteed mathematically to have PMEPRs below a certain value. Chapter Four will summarize certain important results from the literature relating to these *PMEPR reducing codes*.

Chapter Five, containing the main portion of the original research work undertaken for this thesis, will discuss quadrature amplitude modulated (QAM) codes with low PMEPR. We will describe the mathematical properties of complementary QAM sequences, and present and prove properties of two constructions of QAM sequences with low PMEPR—one for the 4-QAM constellation, and the other for the 16-QAM constellation. A special case of the 16-QAM construction gives us complementary sequences in 8-QAM.

We will conclude in Chapter Six by summarizing the contributions of this thesis, and suggesting possible areas for future research.

Chapter 2

Orthogonal Frequency Division Multiplexing (OFDM) Basics

As mentioned in the previous chapter, the basic principle of OFDM is to split a high rate data stream into multiple parallel lower rate data streams, which are block-wise transmitted simultaneously over a number of frequency-spaced subcarriers. As the symbol duration for each of the lower rate subcarriers is increased, the relative dispersion in time caused by multipath delay spread is decreased. The longer symbol duration and the introduction of a *guard time* for every OFDM symbol can eliminate almost completely intersymbol interference. The *cyclic extension* of the OFDM symbol into the guard time ensures the minimization of intercarrier interference. The process of generating an OFDM signal, and the reasoning behind each step will be described in the following sections. The treatment here follows closely that found in [9], pp. 33–51.

2.1 Generation of Basic OFDM Signal Using the IFFT

An OFDM signal consists of a sum of subcarriers that are modulated by using phase shift keying (PSK) or quadrature amplitude modulation (QAM). Other modulation techniques, such as differential schemes, could also be used but for the purposes of this thesis, we will focus on QAM.

Letting $\mathbf{a} = (a_0, a_1, \cdots, a_{n-1})$ be a sequence of complex QAM symbols modulating n subcarriers, T the symbol duration, and f_i's the subcarrier frequencies, then a transmitted OFDM symbol starting at time $t = t_s$ can be written as the real part of the complex

envelope

$$s(t) = \begin{cases} \sum_{i=0}^{n-1} a_i e^{2\pi j f_i (t-t_s)} & t_s \le t \le t_s + T \\ 0 & t < t_s \text{ or } t > t_s + T. \end{cases} \tag{2.1}$$

The carrier frequencies f_i are related by

$$f_i = f + i\Delta f \tag{2.2}$$

where f is the smallest carrier frequency, and Δf is an integer multiple of the OFDM symbol rate, $\frac{1}{T}$. Because the subcarrier spacing is an integer multiple of $\frac{1}{T}$, the envelope of each subcarrier has exactly an integer number of cycles in the symbol interval T. This results in the orthogonality between subcarriers, and is precisely what allows the frequency bands occupied by each subcarrier signal to overlap without causing interference to each other. We will now show how this subcarrier spacing achieves the orthogonality and enables us to demodulate each subcarrier independent of the other subcarriers.

The kth subcarrier from (2.1) is demodulated by downconverting the signal to baseband by multiplying with a frequency of $f_k = f + k\Delta f$ and then integrating the signal over T seconds. [1]

$$\begin{aligned} \int_{t_s}^{t_s+T} e^{-2\pi j f_k (t-t_s)} \sum_{i=0}^{n-1} a_i e^{2\pi j f_i (t-t_s)} dt &= \sum_{i=0}^{n-1} a_i \int_{t_s}^{t_s+T} e^{-2\pi j (i-k)\frac{t-t_s}{T}} dt \\ &= \sum_{i=0}^{n-1} a_i T \delta(i-k) \\ &= a_k T \end{aligned} \tag{2.3}$$

The orthogonality of the OFDM subcarriers can also be seen from the frequency spectra of the subcarriers and how they overlap. Each OFDM symbol is made up of subcarriers that have a constant nonzero envelope over a T-second interval. Thus the spectrum of each subcarrier is a convolution of a Dirac pulse centered at the subcarrier frequency with the spectrum of a rectangular pulse that is non-zero for a T-second period and zero otherwise. Hence, the spectrum for a particular OFDM subcarrier is equal to the product of some constant complex QAM symbol with $\text{sinc}[(f - f_k)T]$, which has zeros for all frequencies f that are a non-zero integer multiple of $\frac{1}{T}$ away from f_k. The overlapping sinc spectra of the

[1] Practical implementation of the demodulation might involve downconverting the *entire* OFDM signal first to an intermediate frequency (for a superheterodyne receiver) or directly to baseband, and then picking out the various subcarriers, instead of downconverting just one particular OFDM subcarrier. Nevertheless, this detail is irrelevant for our purposes.

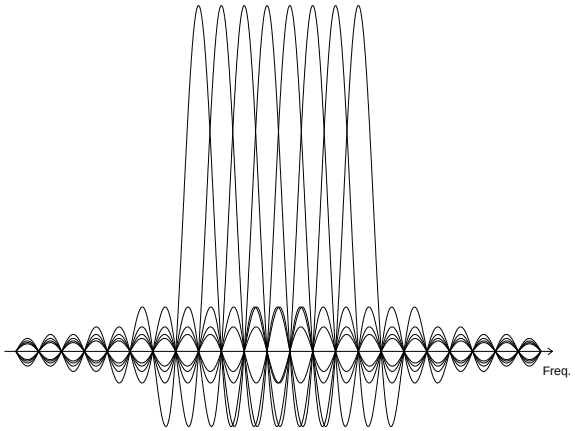

Figure 2-1: Spectra of Individual Subcarriers

individual OFDM subcarriers is shown in Figure 2-1. (Note that the spectra need not have the same amplitude, contrary to what is suggested by the figure.)

Demodulation of the OFDM signal is effectively equivalent to calculating the spectrum values at the points that correspond to the maxima of the individual subcarriers. Since at the maximum of each subcarrier spectrum, all other subcarrier spectra have amplitude zero, we can demodulate each subcarrier free from any interference from the other subcarriers.

Returning to equation (2.1), we can rewrite it as

$$s(t) = \begin{cases} e^{2\pi j f(t-t_s)} \sum_{i=0}^{n-1} a_i e^{2\pi j i \Delta f (t-t_s)} & t_s \le t \le t_s + T \\ 0 & t < t_s \text{ or } t > t_s + T. \end{cases} \tag{2.4}$$

Looking at the complex baseband OFDM signal $\sum_{i=0}^{n-1} a_i e^{2\pi j i \Delta f (t-t_s)}$, we see that it is simply the inverse Fourier transform of the n QAM input symbols. The time discrete equivalent is the N-point inverse discrete Fourier transform (IDFT) given by

$$s_{\text{baseband}}(m) = \sum_{i=0}^{n-1} a_i e^{2\pi j \frac{im}{N}} \tag{2.5}$$

where time t is replaced by sample number m. Note that we use N here instead of n, to suggest that the possibility of oversampling by having $N > n$.

The inverse discrete Fourier transform, in practice, is computed very efficiently using the inverse fast Fourier transform (IFFT) algorithm, and an N-point IFFT using the radix-2 algorithm requires only $\frac{1}{2}N \cdot \log_2 N$ complex multiplications, or only $\frac{3}{8}N\,(\log_2 N - 2)$ complex multiplications using the radix-4 algorithm. This is in contrast to N^2 complex multiplica-

tions for the IDFT. The existence of the IFFT and FFT algorithms with $O(N \log_2 N)$ complexity instead of $O(N^2)$ complexity makes scaling of OFDM systems for higher data rates by increasing the number of subcarriers used per OFDM symbol relatively simple, compared to the $O(N^2)$ complexity of scaling receivers for single-carrier communications systems.

2.2 Guard Time and Cyclic Extension

One of the main motivations behind using OFDM is the efficient way it deals with multipath delay spread. By splitting the input data stream into n parallel streams, the symbol duration can be made n times longer and still achieve the same data rate. This reduces the relative multipath delay spread, relative to the symbol duration, by the same factor n. Now by introducing a guard time to each OFDM symbol, we can eliminate intersymbol interference almost completely.

We choose the guard time (T_G) to be larger than the expected maximum delay spread, so that delayed multipath components of one symbol cannot interfere with the next symbol. Because the relative multipath delay spread is small, the required guard time relative to the symbol duration is also small, thus the spectral efficiency of an OFDM system is not necessarily affected too adversely by the introduction of the guard time.

Since the purpose of the guard times is to ensure that delayed components from the previous symbol do not interfere with the present symbol, i.e. guard the present symbol against interference from the previous symbol, we could think of the guard times as belonging *before* each symbol. A reasonable question to ask at this point is whether we need to transmit any signal at all during the guard time?

Suppose we do not transmit any signal during the guard time. Figure 2-2 depicts such an arrangement. We find that the problem of same-carrier interference and intercarrier interference (ICI) would arise. This is because when we integrate over the symbol period, T_s, we do not integrate over an integer number of cycles for delayed multipath components, whether they are from the same subcarrier or from other subcarriers. Thus the orthogonality property no longer holds. This effect is illustrated in figure 2-2.

To eliminate ICI and same-carrier interference, the OFDM signal is cyclically extended in the guard time. What this means is that we prefix the subcarrier signal with a copy of

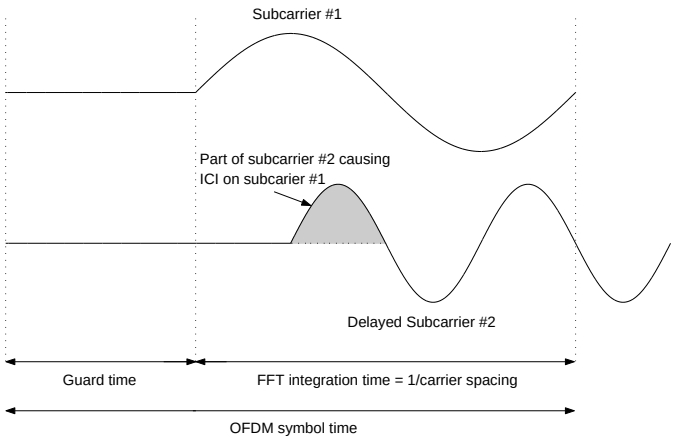

Figure 2-2: Effect of multipath with zero signal in the guard time

the last T_G seconds of the same signal. Since there are an integer number of cycles in the symbol period T_s, the transition at the guard-symbol boundary is guaranteed to be smooth.

This cyclic extension is shown in figure 2-3. It ensures that delayed multipath components of the OFDM symbol always have an integer number of cycles within the FFT interval, as long as the delays are smaller than the guard time. Thus, we have completely eliminated ICI caused by multipath delays smaller than the guard time.

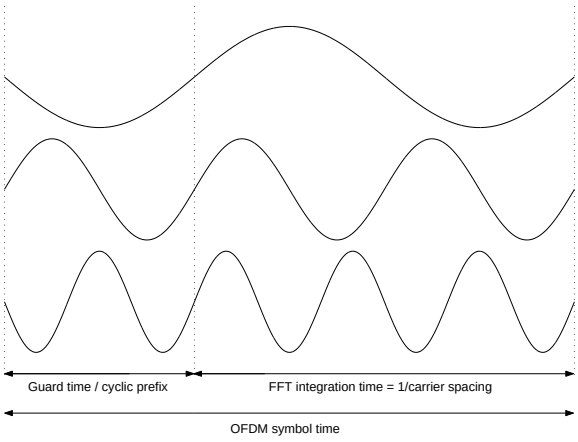

Figure 2-3: OFDM symbol with cyclic extension

Figure 2-4 shows received signals for three subcarriers over three symbol intervals in a two-ray multipath environment. The dashed line represents a delayed multipath component. The OFDM subcarriers in this example are BPSK modulated, and therefore there

can be 180-degree phase jumps at the symbol boundaries. When the delays in multipath components are less than the guard time, phase transitions in the delayed multipath component do not occur during the FFT integration interval, thus allowing the OFDM receiver to "see" the sum of pure sine waves with some phase offsets. Although the sum of multipath components in each subcarrier introduces phase shifts for each subcarrier, orthogonality between the subcarriers is maintained.

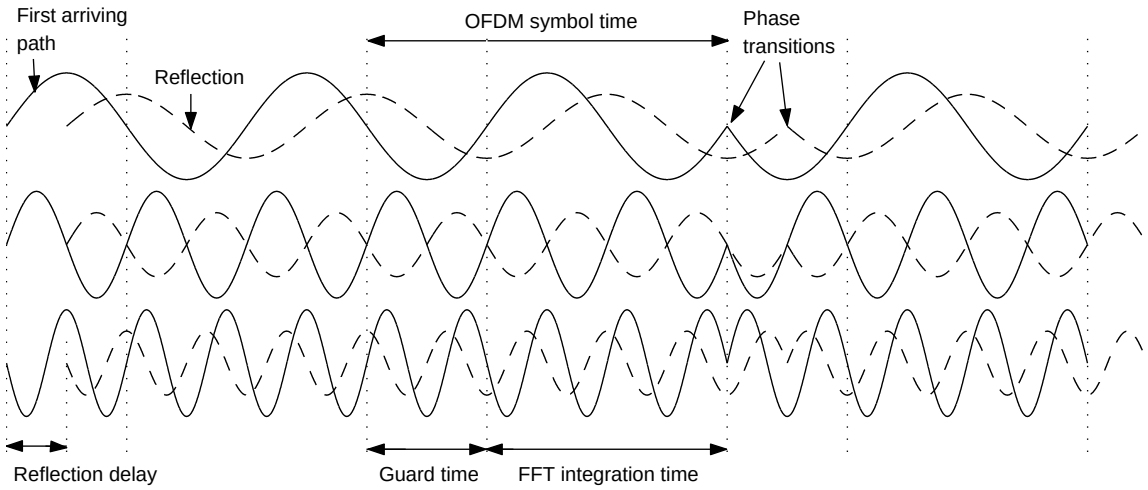

Figure 2-4: Example of an OFDM signal with three subcarriers in a two-ray multipath channel

However, if the multipath delay is greater than the guard time, phase transitions of the delayed paths will fall in the FFT interval. The sum of the signal of the first path with those of delayed paths will no longer be a pure sine wave, and same carrier interference and inter-carrier interference (ICI) would result. Thus in practical implementations, it is important to have a decent estimate of the maximum multipath delay in the environment that the OFDM system is going to be deployed, so that interference of this nature can be minimized.

2.3 Windowing

The sharp phase transitions, as seen at the symbol boundaries in figure 2-4, causes the out-of-band spectrum to decrease rather slowly. To make the spectrum go down more rapidly,

windowing is applied to individual OFDM symbols. Windowing essentially smooths the phase transition between two OFDM symbols. A commonly used window type is the raised cosine window, which is shown in figure 2-5.

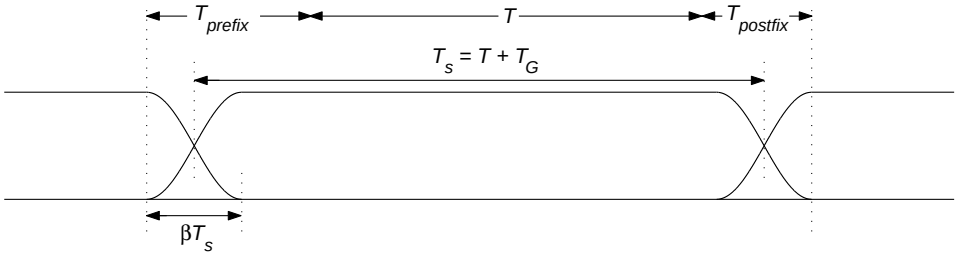

Figure 2-5: Raised cosine window for OFDM showing relative timings for cyclic extension and windowing

The OFDM signal is generated by first padding the n input QAM values with zeros to get N input samples used to calculate the N-point IFFT (oversampling the output). Then, the last T_{prefix} samples of the IFFT output are inserted at the start of the OFDM symbol, and the first T_{postfix} samples are appended at the end. Thus the guard time is now effectively split to occupy both the start and end of the OFDM signal. The OFDM signal is then multiplied by a raised cosine window to more quickly reduce the power of out-of-band frequencies. Finally, the OFDM symbol is added to the output of the previous OFDM symbol with a delay of T_s, such that there is an overlap of βT_s, where β is the rolloff factor of the raised cosine window.

As orthogonality between subcarriers require that amplitude and phase of the subcarriers stay constant during the FFT integration interval of length T, the rolloff region of the window thus decreases the effective guard time by βT_s. Therefore, there is a tradeoff between having a larger rolloff factor, which will suppress the out-of-band spectrum more quickly, and a decreased delay spread tolerance.

2.4 OFDM Receiver Operation

The previous sections have described how the basic OFDM signal is formed by using the IFFT, adding a cyclic extension and then performing windowing. Now, we will discuss briefly the operation of the OFDM receiver. Figure 2-6 shows the basic OFDM transmitter

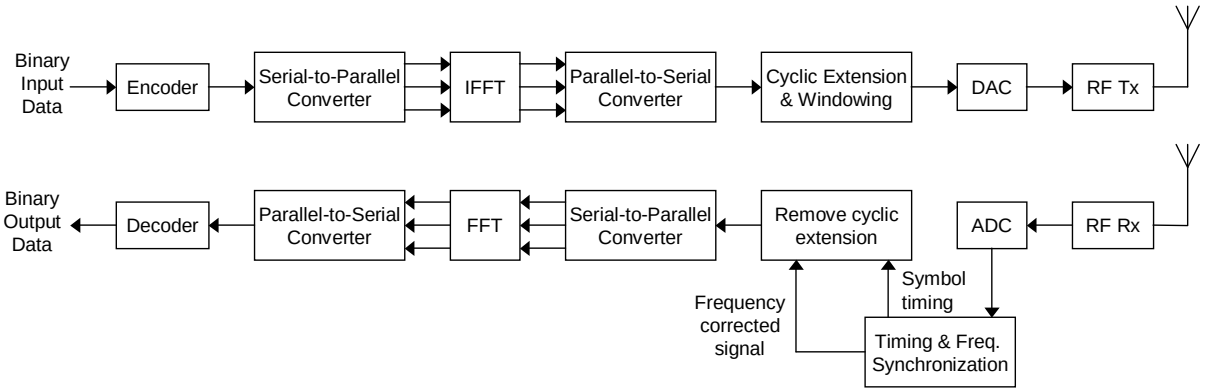

Figure 2-6: Block diagram of an OFDM transceiver

and receiver block diagrams.

For the receiver path, the receiver receives the signal $\mathrm{Re}(s(t))$ perturbed by noise and performs the inverse operations: the RF chain at the receiver down-converts the signal, processes the received data and obtains time-sampled estimates of the signal in digital form. Digital signal processing is used to determine symbol timing and frequency offsets. The receiver then applies a FFT on these estimates and generates $r_0, r_1, \cdots, r_{n-1}$, estimates of $a_0, a_1, \cdots, a_{n-1}$. Mathematically

$$r_i = \alpha_i a_i + \eta_i, \quad i = 0, 1, \cdots, n-1 \tag{2.6}$$

where α_i is a complex number which depends on the channel. Estimates of the channel gain, α_i, are usually obtained through the use of received pilot symbols.

The receiver then extracts the block B_T of input bits by applying a suitable error correction algorithm. Assuming that the receiver has knowledge of the gain coefficients $\alpha_i, i = 0, 1, \cdots, n-1$, the maximum likelihood receiver decides in favor of the codeword $\mathbf{a} = a_0 a_1 \ldots a_{n-1}$ if it minimizes the decision metric

$$\sum_{i=0}^{n-1} |r_i - \alpha_i a_i|^2 \tag{2.7}$$

amongst all possible codewords.

Accurate determination of symbol timing and frequency offsets, and good channel estimation are essential for the successful implementation of OFDM systems, and these are in general non-trivial problems.

We have not discussed encoding and decoding so far. It suffices to mention that there is a myriad of coding techniques and symbol constellations that can be used with OFDM. Of course, the performance of the entire OFDM system will be affected by the coding used. For example, a deep fade affecting a few consecutive subcarriers would result in burst errors in the QAM value output of the FFT for those particular subcarriers. Thus, having interleaving in the coding and decoding processes would spread out the error bits and increase the robustness of the overall code against the burst errors.

This thesis investigates codes that reduce the high peak-to-mean envelope power ratio which is inherent in OFDM signals. The next chapter will define the details of the problem.

Chapter 3

The Peak-to-Mean Envelope Power Ratio (PMEPR) Problem

As an OFDM signal is the result of adding up a number of independently modulated subcarriers, it can have a very large instantaneous power compared to the average power of the signal. The worst case occurs when the signals on the n subcarriers all have the same phase. When added together, the signal has a peak envelope power that is n (or more) times the average envelope power. This effect, for an OFDM signal using a 4-QAM constellation over 16 subcarriers, is illustrated in Figure 3-1.

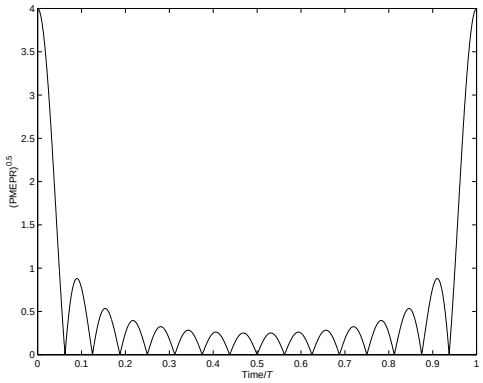

Figure 3-1: Square root of the Peak-to-Mean Envelope Power Ratio for a 16-channel OFDM signal, modulated with the same initial phase for all subchannels

As section 3.2 will show, these high peaks occur rather infrequently, however their presence means that unless we could somehow reduce these peaks, we would have to design our RF power amplifiers to deal with the peaks, even though most of the time, the amplifiers will

be operating in only a fraction of their linear dynamic range. Other than the reduced efficiency of the RF power amplifier, disadvantages of having signals with high PMEPR include the increased complexity required in the analog-to-digital and digital-to-analog converters.

Other concerns such as regulatory limits on the peak power of transmissions, and constraints imposed by battery power limitations in mobile devices, gives us further motivation to find solutions to control the PMEPR of the transmitted OFDM signal.

3.1 Mathematical Definition of PMEPR

We will now define mathematically the Peak-to-Mean Envelope Power Ratio (PMEPR). The PMEPR is defined as follows:

$$PMEPR = \frac{\max_{0\leq t\leq T} |s(t)|^2}{P_{av}} \tag{3.1}$$

where P_{av} is the mean envelope power of an OFDM signal, and the average is taken either over all possible OFDM signals (uncoded), or over all the OFDM signals produced based on some codebook. We consider here the PMEPR for the former case. Let $\mathcal{C}^n$ denote the set of all possible *uncoded* M-QAM sequences of length n. The cardinality of $\mathcal{C}^n$ is M^n.

$$\begin{aligned} P_{av} &= \frac{1}{M^n} \sum_{\mathbf{c}\in\mathcal{C}^n} \frac{1}{T} \int_0^T |s_{\mathbf{c}}(t)|^2 dt \\ &= \frac{1}{M^n} \sum_{\mathbf{c}\in\mathcal{C}^n} \frac{1}{T} \int_0^T \left| \sum_{i=0}^{n-1} c_i e^{2\pi j(f_0+if_\Delta)t} \right|^2 dt \end{aligned}$$

Since the n modulated subcarriers are mutually orthogonal, the integral of the square of the sum of the subcarrier signals is equal to the the sum of the integral of the squares of each subcarrier signal,

$$\begin{aligned} P_{av} &= \frac{1}{M^n} \sum_{\mathbf{c}\in\mathcal{C}^n} \sum_{i=0}^{n-1} \frac{1}{T} \int_0^T \left| c_i e^{2\pi j(f_0+if_\Delta)t} \right|^2 dt \\ &= \frac{1}{M^n} \sum_{\mathbf{c}\in\mathcal{C}^n} \sum_{i=0}^{n-1} |c_i|^2 \\ &= \sum_{i=0}^{n-1} \frac{1}{M^n} \sum_{\mathbf{c}\in\mathcal{C}^n} |c_i|^2 \end{aligned}$$

Now, remembering that $\mathcal{C}^n$ here refers to all possible sequences of the M-QAM symbols, and not just a particular subset, we note that $\frac{1}{M^n}\sum_{\mathbf{c}\in\mathcal{C}^n} |c_i|^2$ is equivalent to the average energy of the symbols in the M-QAM signal constellation, and since we normalize the

average energy of our signal constellations to 1,

$$P_{av} = n \cdot 1 = n. \tag{3.2}$$

Therefore, for M-QAM constellations with unit average energy, taking the average over all possible OFDM signals,

$$PMEPR(\mathbf{c}) = \frac{\max_{0 \le t \le T} |s_{\mathbf{c}}(t)|^2}{n}. \tag{3.3}$$

Lemma 5.6 in chapter 5 will consider the mean envelope power for just a particular subset, and not all possible 16-QAM OFDM signals, and show it to be n as well.

The maximum peak is achieved when all the subcarriers are in phase (i.e. all the c_i's are equal) and the energy of c_i is the largest possible among all symbols. In this case,

$$\begin{aligned} PMEPR_{max}(\mathbf{c}) &= \frac{[n \cdot \max_{c \in \mathcal{C}} |c|]^2}{n} \\ &= n \cdot \max_{c \in \mathcal{C}} |c|^2 . \end{aligned}$$

Thus for the 4-QAM constellation, $PMEPR_{max,4QAM}(\mathbf{c}) = n$, while for the 16-QAM constellation, $PMEPR_{max,16QAM}(\mathbf{c}) = 1.8n$.

3.2 Distribution of the PMEPR

We can look at the distribution of the PMEPR from two perspectives. One is to consider in *time* the probability of the instantaneous envelope power of an OFDM signal being below a certain multiple of the mean envelope power (averaged over all possible OFDM signals). The other is to consider what percentage of *all possible OFDM signals* have a PMEPR less than a certain level. The first perspective is useful in explaining why signal processing techniques to limit PMEPR can be successful in combating the problem without introducing too much distortion. The second perspective provides the rationale for using coding techniques to solve the PMEPR problem.

3.2.1 Distribution in Time

Normalizing so that the average envelope power is 1, we can write the complex baseband OFDM signal as

$$s(t) = \frac{1}{\sqrt{n}} \sum_{i=0}^{n-1} a_i e^{ji\Delta ft}. \tag{3.4}$$

The a_i's are the modulating symbols defined in the signal constellation. From the central limit theorem, it follows that for large values of n, the real and imaginary values of $s(t)$ become Gaussian distributed. The exact mean and variance of the Gaussian distributions depends on the signal constellation. For the rectangular 4-QAM constellation, the Gaussian distributions have mean zero and variance of $1/2$. For the rectangular 16-QAM constellation, with mean energy of 1, the Gaussian distributions also have mean zero and variance of $1/2$. The amplitude of the OFDM signal therefore has a Rayleigh distribution, while the power distribution is a central chi-square distribution with two degrees of freedom and mean one. The cumulative distribution function is given by

$$F(z) = 1 - e^{-z} \tag{3.5}$$

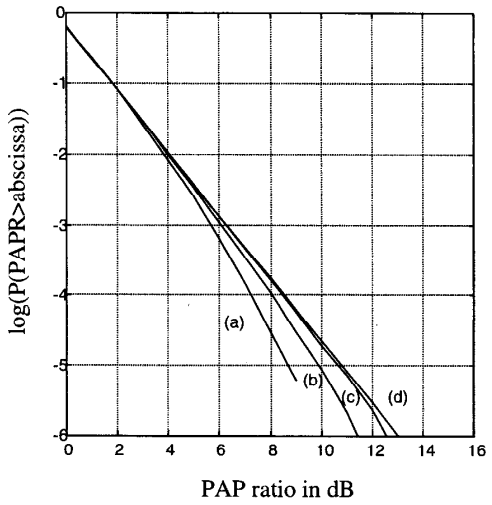

Figure 3-2: Peak-to-Average Power Ratio distribution of an OFDM signal with (a) 12, (b) 24, (c) 48 and (d) an infinite number of subcarriers (pure Gaussian noise). Four times oversampling used in simulation, total number of simulated samples = 12 million.

Figure 3-2 (reproduced from [9], p. 121) shows the probability that the PMEPR (or peak-to-average power ratio, PAPR) exceeds a certain value, by looking at an OFDM signal in time. We see that the curves are close to that for the Gaussian distribution (d) until the peak-to-average power (PAP) value comes within a few dB of the maximum PAP level of $10 \log n$ dB, where n is the number of subcarriers. We also observe that the envelope power of the OFDM signal exceeds four times the mean envelope power less than 0.1 per cent of the time. This suggests that it might be feasible to use signal processing techniques to

control high power peaks as these occur relatively rarely.

3.2.2 Distribution of PMEPR per OFDM Symbol

To derive a mathematical approximation to the cumulative distribution function for the PMEPR per OFDM symbol, we note that for n subcarriers, a non-oversampling IFFT would give us n output values in time. The probability that the PMEPR for an OFDM symbol is below some threshold level z is thus approximately equal to the probability that all n samples in time are below the threshold. (The equality is approximate because the actual peak of the OFDM signal does not necessarily coincide with any of the time-sampled values.) Non-oversampling lets us to assume that the n samples are mutually uncorrelated, hence using the cumulative distribution function for one time sample (3.4), we obtain

$$P(\text{PMEPR} \leq z) = F(z)^n = \left[1 - e^{-z}\right]^n. \tag{3.6}$$

Figure 3-3 ([9], p. 122) plots the theoretical derivation of the cumulative distribution function and values obtained from simulations for various values of n.

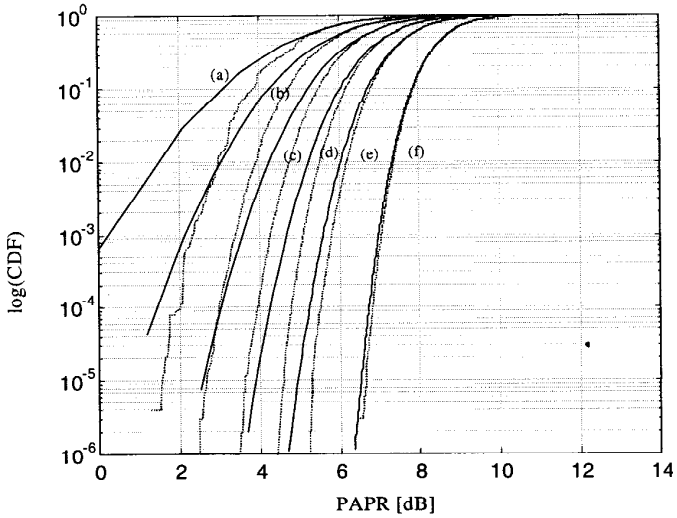

Figure 3-3: PMEPR distribution without oversampling for (a) 16, (b) 32, (c) 64, (d) 128, (e) 256, and (f) 1024 subcarriers (dotted lines are simulated).

To obtain a better approximation of the cumulative distribution function, we might consider applying oversampling when performing the IFFT. However, oversampling means that the time-sampled values are no longer mutually uncorrelated, and we cannot make use of this assumption in deriving the distribution function. Van Nee and Prasad [9] propose

an approximation by assuming that the distribution for n subcarriers and oversampling can be approximated by the distribution for αn subcarriers without oversampling, with α larger than one. Hence, the effect of oversampling is approximated by adding a certain number of extra samples. The distribution of the PMEPR is then given by

$$P(\text{PMEPR} \leq z) = F(z)^{\alpha \cdot n} = \left[1 - e^{-z}\right]^{\alpha \cdot n}. \tag{3.7}$$

Figure 3-4 ([9], p. 123) plots the PMEPR distribution given by equation (3.7), where $\alpha = 2.8$. The dotted lines are curves obtained from simulations. We see that equation (3.7) is quite accurate for $n > 64$. Equation (3.6), however, gives a better approximation for large values of the cumulative distribution function (> 0.5).

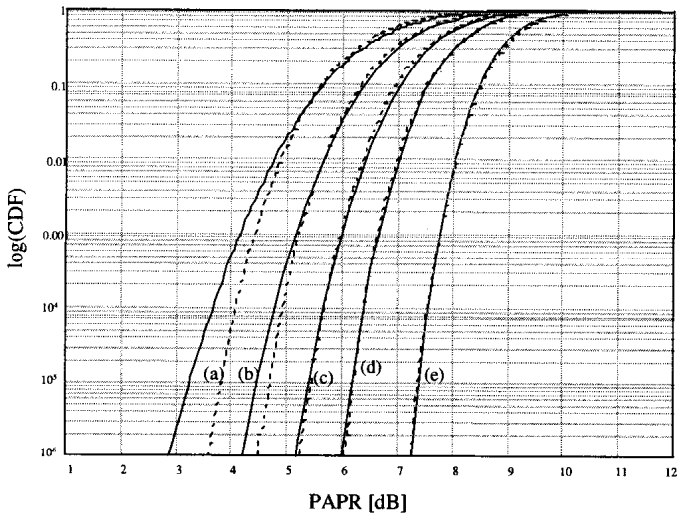

Figure 3-4: PMEPR distribution with oversampling ($\alpha = 2.8$) for (a) 32, (b) 64, (c) 128, (d) 256, and (e) 1024 subcarriers (dotted lines are simulated).

Figure 3-4 suggests that it might be feasible to use coding techniques to reduce the PMEPR, as reasonable coding rates are possible for a PMEPR of around 4 to 6 dB. For example, in the case of 64 subcarriers, about 10^{-6} of all possible QPSK sequences have a PMEPR of less than 4.2 dB. This means that only 20 out of a total of 128 bits would be lost if only the sequences with a low PMEPR were used in our codebook. However, the main practical difficulty in this approach is in finding a coding scheme with a reasonable coding rate (large enough code size) that produces only OFDM signals with low PMEPR, and also has reasonable error correcting properties. The main thrust of the research for this thesis is in uncovering such coding schemes for OFDM signals based on QAM sequences.

3.3 Solutions to the PMEPR Problem

As solving the PMEPR problem would have significant implications to the widespread practical applicability of OFDM, it has been an area of active research. Several approaches to alleviate the PMEPR problem exist, and these may be broadly grouped into two categories, the first being signal processing techniques that reduce the PMEPR after the Fourier transform is performed. Section 3.2.1 showed that large PMEPRs occur relatively infrequently, thus it is possible to remove these peaks at the cost of introducing a small amount of self-interference. The challenge of using signal processing techniques to remove high peaks is to keep the spectral pollution caused by this distortion as low as possible. Signal processing techniques to reduce the PMEPR include clipping and windowing, and peak cancellation. The second category consists of using codes that after undergoing the IFFT produce signals that have a limited PMEPR. We will examine briefly here the first category of techniques, and in the next chapter, discuss in detail codes that reduce the PMEPR.

3.3.1 Clipping and Peak Windowing

Clipping is simply limiting the signal to a desired maximum level, when the signal amplitude exceeds the maximum. This is the simplest solution. The disadvantages of clipping are that it introduces nonlinear distortion to the OFDM signal, and significantly increases the level of out-of-band radiation.

Peak windowing is less crude than clipping in that instead of chopping off large signal peaks, the peaks are multiplied with non-rectangular windows with good spectral properties, such as the raised cosine, Kaiser, and Hamming windows.

Figure 3-5 ([9], p. 124) gives an example of using windowing to reduce large power peaks in an OFDM signal.

Figure 3-6 ([9], p. 125) shows the difference between clipping a signal and peak windowing it. Figure 3-7 ([9], p. 125) demonstrates how the spectral distortion can be decreased by increasing the window width.

3.3.2 Peak Cancellation

Instead of *multiplying* large peaks by windows which scale the amplitude by a factor less than one, we can reduce the peak power by *subtracting* off peaked delta-like signal functions

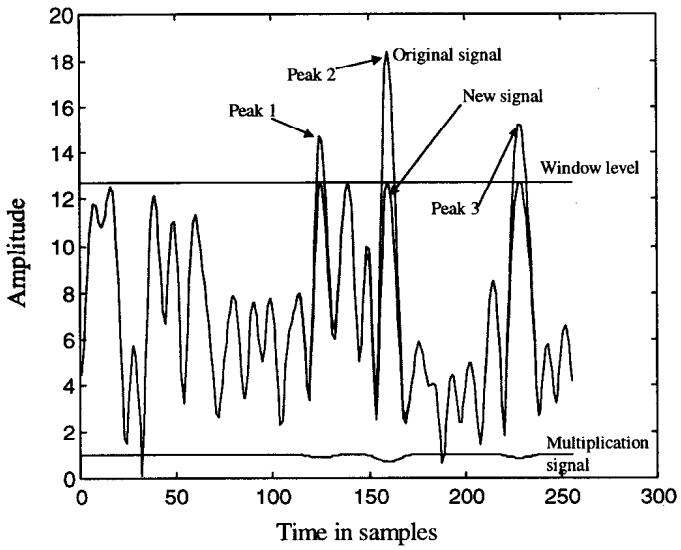

Figure 3-5: Windowing an OFDM time signal

which are band-limited to the bandwidth of the transmitted OFDM signal. This method is known as peak cancellation. A suitable signal for this purpose is a sinc function, since it is bandlimited. However since a sinc function has infinite time support, for practical purposes, we multiply the sinc function in time by a time-limited raised cosine window, and subtract scaled versions of this function one or more times to reduce peaks exceeding a certain threshold to the desired maximum level.

We find that peak cancellation introduces minimal spectral distortion compared to clipping and peak windowing. This is achieved at the expense of a time delay equivalent to half the duration of the peak-cancelling time-limited sinc function.

Figures 3-8 and 3-9 ([9], p. 135) show an example of peak cancellation in the time domain. In this example, because one sinc function is not wide enough to reduce the peak, the cancellation signal actually consists of two separate sinc functions. Figure 3-10 shows the effect of peak cancellation on the power spectral density of the OFDM system compared to clipping. We see that when peak cancellation is applied to an OFDM system with worst case PMEPR of 15 dB, negligible distortion in the frequency domain is introduced, while the PMEPR is reduced to 4 dB. This is in contrast to clipping (applied to reduce PMEPR to 4 dB) which causes significant spectral distortion. The reader is referred to [9], pp. 131-138 for more details.

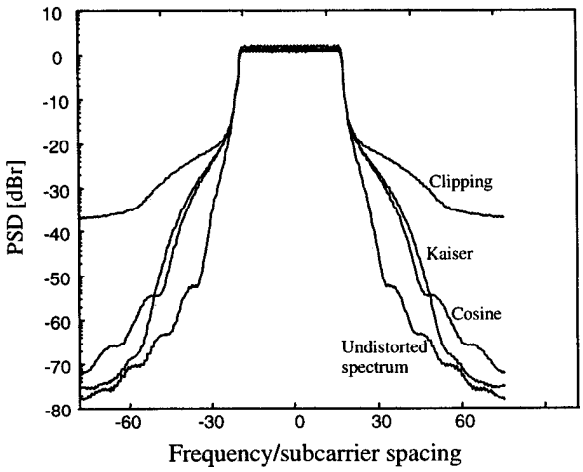

Figure 3-6: Frequency spectrum of an OFDM signal with 32 subcarriers with clipping and peak windowing at a threshold level of 3 dB above the rms amplitude

3.3.3 Other Solutions

Other than signal processing and coding techniques (which we will investigate further in subsequent chapters), there are various other novel methods to reduce the PMEPR, and these are probably best characterized as hybrid methods involving both coding and signal processing. Examples include symbol scrambling, phase rotation and constellation shaping. We will not discuss these techniques here, and the reader is referred to current literature for the latest developments in attempts to solve the PMEPR problem.

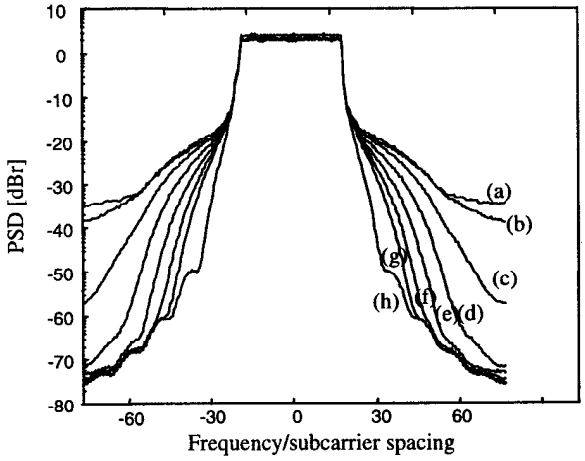

Figure 3-7: Frequency spectrum of an OFDM signal with 32 subcarriers with peak windowing at a threshold level of 3 dB above the rms amplitude. Symbol length is 128 samples (4 times oversampled) and window length is (a) 3, (b) 5, (c) 7, (d) 9, (e) 11, (f) 13, and (g) 15 samples. Curve (h) is the ideal OFDM spectrum.

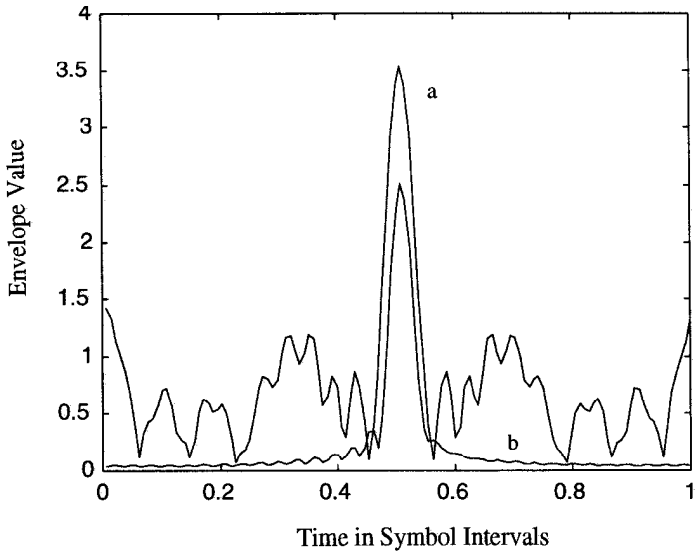

Figure 3-8: (a) OFDM symbol envelope, (b) cancellation signal envelope

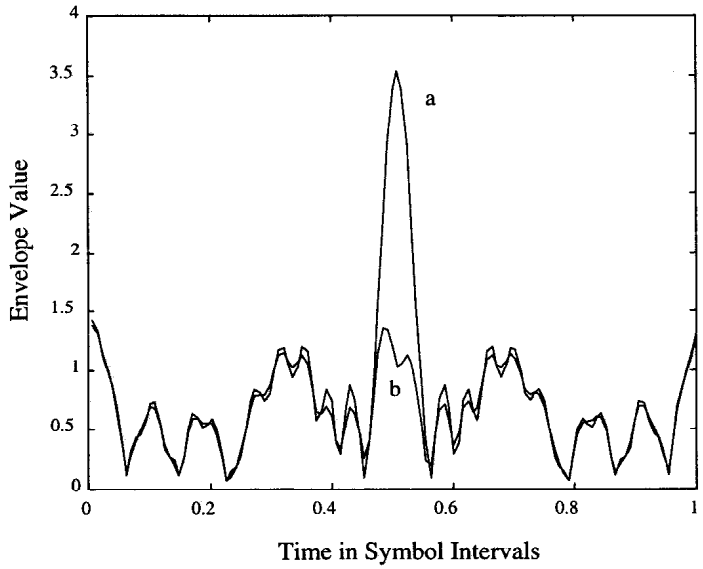

Figure 3-9: (a) OFDM symbol envelope, (b) signal envelope after peak cancellation

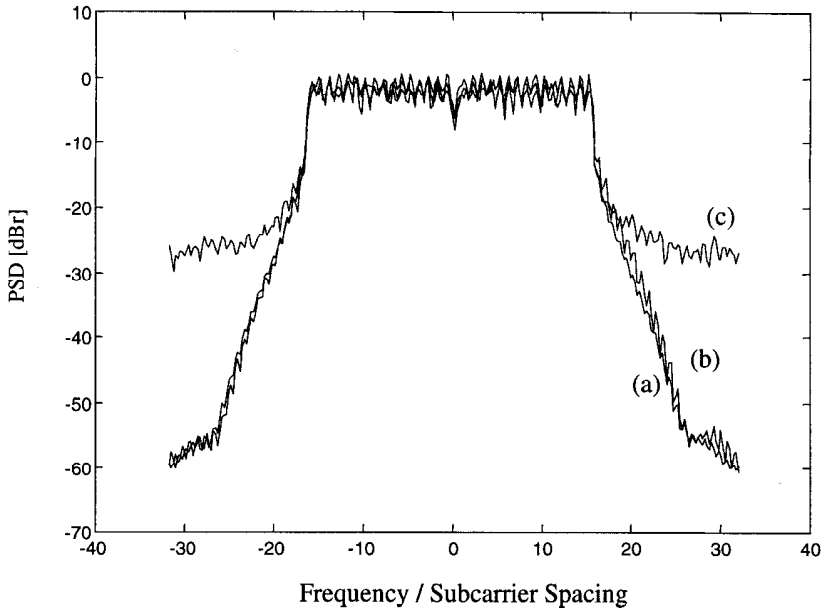

Figure 3-10: Power spectral density for (a) undistorted spectrum with 32 subcarriers, PMEPR = 15 dB, (b) spectrum after peak cancellation to PMEPR = 4 dB, and (c) clipping to PMEPR = 4 dB. Reference cancellation function has a length equal to 1/4 of the length of an OFDM symbol

Chapter 4

PMEPR Reducing Codes

The idea of PMEPR reducing codes is based on the fact that among all possible input sequences, there are certain sequences which after undergoing the inverse Fourier transform operation will result in signals that have low PMEPR. By finding a code structure within these low PMEPR sequences, it might be possible to use the code to combine forward error correction with a reduction in PMEPR.

Also, there is a large practical advantage in using structured sets of low PMEPR sequences (i.e. codes) as opposed to just using a list of such sequences found by a computer search. Whereas computer generated lists of sequences have to be encoded, in general, by table-lookup techniques, structured sets of low PMEPR sequences admit a more compact description which can be exploited in the encoding as well as the decoding stage. [8]

Let us now examine further mathematically some properties that a low PMEPR sequence would have to satisfy. The treatment below will follow closely the approach taken in [1].

Recall from section 2.1 that the transmitted OFDM signal is the real part of the complex signal

$$s(t) = \sum_{i=0}^{n-1} a_i(t) e^{2\pi j f_i t} \tag{4.1}$$

where f_i is the frequency of the ith carrier and $a_i(t)$ is constant over a symbol period. To ensure orthogonality, the carrier frequencies are related by

$$f_i = f + i\Delta f \tag{4.2}$$

where f is the smallest carrier frequency, and Δf is an integer multiple of the OFDM symbol rate (inverse of the OFDM symbol period). The *instantaneous envelope power* of

$s(t)$ is the real-valued function $P(t) = |s(t)|^2$. Substituting from (4.1) and (4.2) gives

$$\begin{aligned} P(t) &= s(t)s^*(t) \\ &= \left(\sum_{i=0}^{n-1} a_i(t)e^{2\pi j f_i t}\right)\left(\sum_{k=0}^{n-1} a_k^*(t)e^{-2\pi j f_k t}\right) \\ &= \sum_{i=0}^{n-1}\sum_{k=0}^{n-1} a_i(t)a_k^*(t)e^{2\pi j(i-k)\Delta f t}. \end{aligned} \tag{4.3}$$

Let a_i denote the constant value of $a_i(t)$ over a symbol period, and the envelope power $P_{\mathbf{a}}(t)$ of the sequence $\mathbf{a} = (a_0, a_1, \cdots, a_{n-1})$ denote the continuous function $P(t)$ over the symbol period. Putting $k = i + u$ in the expression for $P_{\mathbf{a}}(t)$ given by (4.3) we obtain

$$\begin{aligned} P_{\mathbf{a}}(t) &= \sum_u \sum_i a_i a_{i+u}^* e^{2\pi j u \Delta f t} \\ &= \sum_{i=0}^{n-1} |a_i|^2 + \sum_{u\neq 0}\sum_i a_i a_{i+u}^* e^{2\pi j u \Delta f t}, \end{aligned} \tag{4.4}$$

where here and in (4.5) below the summations are understood to be over only those integer values for which both i and $i+u$ lie within $0, 1, \cdots, n-1$. Defining P_A to equal $\sum_{i=0}^{n-1} |a_i|^2$, and the aperiodic autocorrelation of sequence a at delay-shift u to be

$$C_{\mathbf{a}}(u) = \sum_i a_i a_{i+u}^*, \tag{4.5}$$

we can rewrite (4.4) as

$$P_{\mathbf{a}}(t) = P_A + \sum_{u\neq 0} C_{\mathbf{a}}(u) e^{2\pi j u \Delta f t}. \tag{4.6}$$

We will now examine a particular subset of sequences with a property which exploits the expression for $P_{\mathbf{a}}(t)$ in (4.6) to enable us to obtain a good upper bound to $P_{\mathbf{a}}(t)$.

4.1 Golay Complementary Sequences

Golay complementary sequences are so named because it was Marcel J. E. Golay who first wrote about their properties in great detail in 1961 [3]. Golay complementary pairs are pairs of sequences (termed *Golay complementary sequences*, or *complementary sequences* in short) for which the sum of the aperiodic autocorrelation functions is zero for all delay shifts, u, not equal to zero. Mathematically, a sequence $\mathbf{x} = (x_0, x_1, \cdots, x_{n-1})$ of length n

is said to be (Golay) complementary to another sequence $\mathbf{y}$,[1] if the sequences satisfy the following condition:

$$\sum_{0\le i,i+u\le n-1} x_i x_{i+u}^* + \sum_{0\le i,i+u\le n-1} y_i y_{i+u}^* = \begin{cases} P_X + P_Y & u = 0 \\ 0 & u \neq 0. \end{cases} \tag{4.7}$$

Although Golay considered only binary complementary sequences where x_i's and y_i's could take only values of $+1$ or -1, we have extended Golay's original complementarity condition so that we can apply it to sequences made up from complex symbols.

Using the notation introduced in (4.5), the complementarity condition is equivalent to

$$C_{\mathbf{x}}(u) + C_{\mathbf{y}}(u) = \begin{cases} P_X + P_Y & u = 0 \\ 0 & u \neq 0. \end{cases} \tag{4.8}$$

Now, we are ready to prove an upper bound for the PMEPR of Golay sequences.

Theorem 4.1 *The PMEPR of any Golay sequence* $\mathbf{a}$ *with complementary pair* $\mathbf{b}$ *with symbols taken from a constellation with unit average energy is at most* $\frac{1}{n}(P_A + P_B)$.

Proof: Let $\mathbf{a}$ and $\mathbf{b}$ be a Golay complementary pair, so that by definition $C_{\mathbf{a}}(u)+C_{\mathbf{b}}(u) = 0$ for all $u \neq 0$. Then from (4.6), $P_{\mathbf{a}}(t) + P_{\mathbf{b}}(t) = P_A + P_B$, and since $P_{\mathbf{b}}(t) = |s_b(t)|^2 \geq 0$, we deduce that $P_{\mathbf{a}}(t) \leq P_A + P_B$. The result follows from (3.3). □

Corollary 4.2 *For constellations in which all symbols have unit power, the PMEPR of any Golay sequence is at most* 2.

Proof: Using Theorem 4.1, and noting that for constellations in which all symbols have unit power, $P_A = P_B = n$, the result follows immediately. □

We have thus shown that Golay complementary sequences have desirable PMEPR properties. However, the theorem does not tell us how these sequences are distributed, or whether there is a coding structure associated with the sequences. This leads us to a relatively recent result of Davis and Jedwab, linking Golay complementary sequences with Reed-Muller codes.

[1] Clearly, $\mathbf{y}$ must also be of length n, since supposing $\mathbf{y}$ is of length $m > n$, and the first and last $m-n$ symbols in y are not all zeroes (else $\mathbf{y}$ effectively becomes a length n sequence), then the autocorrelation function of $\mathbf{x}$ for delay shift $m-1$ is zero, while that of $\mathbf{y}$ is non-zero, meaning $\mathbf{x}$ and $\mathbf{y}$ cannot be complementary.

4.2 Golay Complementary Sequences and Reed-Muller Codes

Davis and Jedwab demonstrated in [1] a previously unrecognized connection between Golay complementary sequences and second-order Reed-Muller codes over 2^h-PSK constellations. This result was later generalized by Paterson [4] to q-ary polyphase constellation for even q. For our purposes, the results of Davis and Jedwab for 2^h-PSK constellations suffice, and we will discuss here a condensed version of their results.

4.2.1 Boolean Functions and Reed-Muller Codes

In order to present Davis and Jedwab's theorem, let us first define the first and second order binary Reed-Muller codes. Let $x_1, x_2, \cdots, x_m$ denote $\{0,1\}$ valued variables. A Boolean function $f(\cdot,\cdot,\cdots,\cdot)$ of these m variables is a mapping $\{0,1\}^m \rightarrow \mathbb{Z}_2$. It is well-known that any Boolean function in these m variables can be written in algebraic normal form as the sum of constant function 1 (zero-th order monomial) and monomials of the form $x_{j_1}x_{j_2}\cdots x_{j_r}$, with order r ranging from 1 to m, and $1 \leq j_1, \cdots, j_r \leq m$ being distinct numbers. With any Boolean function $f(\cdot,\cdot,\cdots,\cdot)$ in these m variables, one can identify a length 2^m $\mathbb{Z}_2$-valued vector $\mathbf{f} = (f_0, f_1, \cdots, f_{2^m-1})$ in which $f_i = f(i_1, i_2, \cdots, i_m)$ where $i_1 i_2 \cdots i_m$ is the binary expansion of integer i, i.e. $i = \sum_{k=1}^{m} i_k 2^{m-k}$. For example, for $m = 3$, we have

$$\mathbf{f} = (f(0,0,0), f(0,0,1), f(0,1,0), f(0,1,1), f(1,0,0), f(1,0,1), f(1,1,0), f(1,1,1))$$

and so $\mathbf{1} = (11111111)$, $\mathbf{x}_1 = (00001111)$, $\mathbf{x_2} = (00110011)$, $\mathbf{x_3} = (01010101)$, and $\mathbf{x_1x_2} + \mathbf{x_2x_3} = (00010010)$.

We define a *generalized Boolean function* to be a function f from $\mathbb{Z}_2^m$ to $\mathbb{Z}_{2^h}$, where $h \geq 1$. It can be shown that any such function can be uniquely expressed as a linear combination over $\mathbb{Z}_{2^h}$ of the monomials described above (1, x_1, x_2, $\cdots$, x_m, x_1x_2, x_1x_3, $\cdots$, $x_{m-1}x_m$, $\cdots$, $x_1x_2\cdots x_m$) where the coefficient of each monomial belongs to $\mathbb{Z}_{2^h}$. As above, we specify a sequence $\mathbf{f}$ of length 2^m corresponding to the generalized Boolean function f. For example, for $h = 2$ and $m = 3$, we have $2\mathbf{x_1} = (00002222)$, $3\mathbf{x_1x_2x_3} = (00000003)$, and $\mathbf{x_2x_1} + 2\mathbf{x_1x_3} + 3\cdot\mathbf{1} = (33333102)$. Technically, for such expressions to be valid, the range space $\mathbb{Z}_2^{2^m}$ of the monomials should be embedded in $\mathbb{Z}_{2^h}^{2^m}$.

Since there is a one-to-one mapping between the (generalized) Boolean function f and the sequence $\mathbf{f}$ of length 2^m, we shall use f to refer to both the Boolean function and the

sequence $\mathbf{f}$.

The first order Reed-Muller code $RM(1,m)$ is defined to be the set of Boolean functions generated by the zero-th order constant monomial 1 and first order monomials $x_1, x_2, \cdots, x_m$. The second order Reed-Muller code $RM(2,m)$ is defined to be the set of Boolean functions generated by the zero-th order monomial 1, the first order monomials $x_1, x_2, \cdots, x_m$ and the second order monomials $x_{j_1}x_{j_2}$ for $0 \leq j_1 \neq j_2 \leq m-1$.

Let $\xi = \exp\left(\frac{j\pi}{2^{h-1}}\right)$, and $g(i) = \xi^i$ for $i \in \mathbb{Z}_{2^h}$. When $h = 1$, $g(\cdot)$ maps $\{0,1\}$ to the BPSK constellation $\{+1,-1\}$. And when $h = 2$, $g(\cdot)$ maps $\mathbb{Z}_4$ to the QPSK constellation $\{+1,+j,-1,-j\}$. By a slight abuse of notation, for any Boolean function $f = (f_0, f_1, \cdots, f_{2^m-1})$, we define $g(f)$ to be the vector $(g(f_0), g(f_1), \cdots, g(f_{2^m-1}))$. Thus $g(\cdot)$ maps binary vectors into BPSK sequences, and vectors in $\mathbb{Z}_4$ into QPSK sequences. If S denotes a set of Boolean functions, then we define $g(S) = \{g(f) \mid f \in S\}$.

4.2.2 Theorem of Davis and Jedwab

We now present Davis and Jedwab's theorem:

Theorem 4.3 *Let π denote any permutation of the set $1, 2, \cdots, m$. Then any element $\mathbf{c}$ of $g\left(RM(1,m) + 2^{h-1}\sum_{k=1}^{m-1} x_{\pi(k)}x_{\pi(k+1)}\right)$ is a Golay complementary 2^h-ary PSK sequence of length 2^m.*

This result relates a subset of Golay complementary sequences of length 2^m to the well-understood Reed-Muller (RM) code structure. Not only is the encoding based on Davis and Jedwab's description simple, the RM code structure allows for the adaptation of existing decoding techniques already known for RM-codes to be used for these Golay complementary sequences. It is also straightforward to deduce the code set sizes, and distance properties for these subsets of Golay complementary sequences as they are first order cosets of second order RM codes.

The proof is replicated here for completeness. We will be using this theorem and ideas contained in the proof extensively in chapter 5.

Proof: Let

$$f(x_1, x_2, \cdots, x_m) = 2^{h-1}\sum_{k=1}^{m-1} x_{\pi(k)}x_{\pi(k+1)} + \sum_{k=1}^{m} c_k x_k \tag{4.9}$$

where π is a permutation of the symbols $\{1, 2, \cdots, m\}$ and $c_k \in \mathbb{Z}_{2^h}$. We will show that the images $g(a)$ and $g(b)$ for

$$a(x_1, x_2, \cdots, x_m) = f(x_1, x_2, \cdots, x_m) + c$$

and

$$b(x_1, x_2, \cdots, x_m) = f(x_1, x_2, \cdots, x_m) + 2^{h-1} x_{\pi(1)} + c'$$

form a Golay complementary pair over $\mathbb{Z}_{2^h}$ of length 2^m for any c, $c' \in \mathbb{Z}_{2^h}$. The sequences described by a form cosets of $\mathrm{RM}(1, m)$ in $\mathrm{RM}(2, m)$ with coset representative $2^{h-1} \sum_{k=1}^{m-1} x_{\pi(k)} x_{\pi(k+1)}$, and thus the theorem would follow immediately.

The case $m = 1$ can be easily verified by explicit computation, and is in fact trivial, since any length 2 sequence (α_0, α_1) is complementary with the sequence $(\alpha_0, -\alpha_1)$. So we assume $m \geq 2$ and fix $u \neq 0$. By the definitions of aperiodic correlation (4.5) and the mapping $g(a_0, a_1, \cdots, a_{2^m-1}) = (\xi^{a_0}, \xi^{a_1}, \cdots, \xi^{a_{2^m-1}})$, $C_a(u) + C_b(u)$ is the sum over i of terms $\xi^{a_i - a_{i+u}} + \xi^{b_i - b_{i+u}}$, where $\xi = \exp(\frac{j\pi}{2^{h-1}})$, a primitive 2^h-th root of unity. For a given integer i, set $j = i+u$ and let $(i_1, i_2, \cdots, i_m)$ and $(j_1, j_2, \cdots, j_m)$ be the binary representation of i and j respectively. The sequence element a_i is given by $a(i_1, i_2, \cdots, i_m)$ as discussed above, which implies that

$$b_i - a_i \quad = \quad 2^{h-1} i_{\pi(1)} + c' - c \tag{4.10}$$

Case 1: $j_{\pi(1)} \neq i_{\pi(1)}$. From (4.10), over $\mathbb{Z}_{2^h}$, we have

$$a_i - a_j - b_i + b_j = 2^{h-1} \left(j_{\pi(1)} - i_{\pi(1)} \right) = 2^{h-1}$$

so

$$\xi^{a_i - a_j} / \xi^{b_i - b_j} = \xi^{2^{h-1}} = -1.$$

Therefore, $\xi^{a_i - a_{i+u}} + \xi^{b_i - b_{i+u}} = 0$.

Case 2: $j_{\pi(1)} = i_{\pi(1)}$. Since $j \neq i$ we can define v to be the smallest integer for which $i_{\pi(v)} \neq j_{\pi(v)}$. Let i' be the integer whose binary representation

$$(i_1, i_2, \cdots, 1 - i_{\pi(v-1)}, \cdots, i_m)$$

differs from that of i only in position $\pi(v-1)$, so similarly let j' have binary representation

$$(j_1, j_2, \cdots, 1 - j_{\pi(v-1)}, \cdots, j_m).$$

By assumption $i_{\pi(v-1)} = j_{\pi(v-1)}$ and so $j' = i' + u$. We have, therefore, defined an invertible map from the ordered pair (i, j) to (i', j'), and both pairs contribute to $C_a(u) + C_b(u)$. Now substitution for i and i' in (4.9) gives

$$f_{i'} - f_i = 2^{h-1} i_{\pi(v-2)} + 2^{h-1} i_{\pi(v)} + c_{\pi(v-1)} - 2c_{\pi(v-1)} i_{\pi(v-1)}$$

(unless $v = 2$, in which case we just delete terms involving $\pi(v-2)$ here and in what follows). Therefore,

$$\begin{aligned} a_i - a_j - a_{i'} + a_{j'} &= 2^{h-1}\left(j_{\pi(v-2)} - i_{\pi(v-2)}\right) + 2^{h-1}\left(j_{\pi(v)} - i_{\pi(v)}\right) \\ &\quad -2c_{\pi(v-1)}\left(j_{\pi(v-1)} - i_{\pi(v-1)}\right) \\ &= 2^{h-1} \end{aligned}$$

by the definition of v. Then (4.10) implies that

$$b_i - b_j - b_{i'} + b_{j'} = a_i - a_j - a_{i'} + a_{j'} = 2^{h-1}.$$

Arguing as in case 1, we obtain

$$\xi^{a_i - a_j} + \xi^{a_{i'} - a_{j'}} = 0$$

and

$$\xi^{b_i - b_j} + \xi^{b_{i'} - b_{j'}} = 0.$$

Therefore, $\left(\xi^{a_i - a_j} + \xi^{b_i - b_j}\right) + \left(\xi^{a_{i'} - a_{j'}} + \xi^{b_{i'} - b_{j'}}\right) = 0.$

Combining these cases we see that $C_a(u) + C_b(u)$ comprises zero contributions (as in case 1), and contributions which sum to zero in pairs (as in case 2). Therefore, $g\left(a(x_1, x_2, \cdots, x_m)\right)$ and $g\left(b(x_1, x_2, \cdots, x_m)\right)$ are a Golay complementary pair, by the definition expressed in (4.8).

Corollary 4.4 *For any permutation π of the symbols $\{1, 2, \cdots, m\}$ and for any c, $c_k \in \mathbb{Z}_{2^h}$*

$$a(x_1, x_2, \cdots, x_m) = 2^{h-1} \sum_{k=1}^{m-1} x_{\pi(k)} x_{\pi(k+1)} + \sum_{k=1}^{m} c_k x_k + c$$

is a Golay complementary sequence over $\mathbb{Z}_{2^h}$ of length 2^m.

Corollary 4.4 explicitly determines $2^{h(m+1)} \cdot m!/2$ Golay complementary sequences over $\mathbb{Z}_{2^h}$ of length 2^m (using the factor $m!/2$ rather than $m!$ because the expression $\sum_{k=1}^{m-1} x_{\pi(k)} x_{\pi(k+1)}$ is invariant under the mapping $\pi \mapsto \pi'$, where $\pi'(k) = \pi(m + 1 - k)$).

The reader is directed to [1] for more details on the properties of the Reed-Muller code laid out above and further generalizations of theorem 4.3.

Chapter 5

Quadrature Amplitude Modulated (QAM) Codes with Low PMEPR

We have seen in the previous chapter that Golay complementary sequences have good autocorrelation properties which make them good candidates for use as OFDM codes with low peak to mean envelope power ratio (PMEPR).

As we try to squeeze more throughput through our channel while using the same bandwidth, it is natural to extend our signal constellation from using binary signals (BPSK) to using constellations of higher orders, e.g. 4-PSK, 16-QAM, 64-QAM, etc.

Sivaswamy [7], Frank [2], Urbanke and Krishnakumar [8], Davis and Jedwab [1], Paterson [4] and others have extended Golay's results for complementary sequences from binary to polyphase, or phase shift keying (PSK), constellations. However, there has been a gap in the literature on complementary sequences based on quadrature amplitude modulated (QAM) constellations. This thesis attempts to fill this gap.

Section 5.1 clarifies the QAM constellations we are considering, defines the notation that we will be using, and explains the notion of complementarity for QAM sequences. Section 5.2 describes properties of QAM complementary sequences. Most, if not all, of the results presented are applicable to 4-QAM, 16-QAM,, 64-QAM, and other QAM constellations which are centered about the origin and form a square lattice. This section closely parallels Golay's paper on binary complementary sequences [3].

5.1 Preliminaries

5.1.1 Constellations for Quadrature Amplitude Modulation

Figure 5-1 describes graphically the 4-QAM, 16-QAM, and 64-QAM signal constellations, a few examples of the rectangular QAM constellations that we are referring to when we discuss, in general, QAM constellations. Common characteristics of these QAM constellations

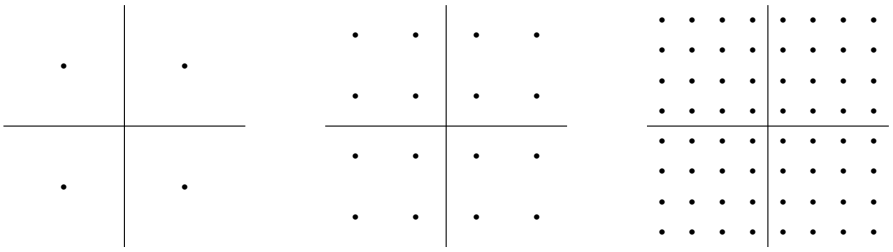

Figure 5-1: 4-QAM, 16-QAM, and 64-QAM signal constellations

are that they are square lattices with the symbols equally spaced from their neighbors. We also note the rotational and reflective symmetries of these constellations.

5.1.2 Notation and Definitions

Following the notation in the previous chapters, we will still use $\mathbf{a}$ and $\mathbf{b}$ to denote a pair of complementary QAM sequences of length n. Thus $\mathbf{a}$ can be written as $(a_0 a_1 \dots a_{n-1})$, and $\mathbf{b}$ as $(b_0 b_1 \dots b_{n-1})$.

We will define the autocorrelation function of a sequence $\mathbf{a}$ as

$$C_{\mathbf{a}}(u) = \sum_{0 \le i, i+u \le n-1} a_i a_{i+u}^*$$

and the power of a sequence $\mathbf{a}$ as

$$P_A = C_{\mathbf{a}}(0) = \sum_{i=0}^{n-1} a_i a_i^*$$

The necessary and sufficient condition for $\mathbf{a}$ and $\mathbf{b}$ to be a pair of complementary sequences is for

$$C_{\mathbf{a}}(u) + C_{\mathbf{b}}(u) = (P_A + P_B)\delta(u),$$

where

$$\delta(u) = \begin{cases} 1 & \text{for } u = 0 \\ 0 & \text{otherwise} \end{cases}$$

Note that $P_A + P_B$ is generally different for different complementary pairs formed from the same QAM constellation. Hence, corollary 4.2 (which states that the PMEPR bound is 2 for Golay complementary sequences formed from equal energy constellations) does not hold for QAM constellations, since in general QAM symbols have different energy. However if the constellation is normalized to have unit average energy, theorem 4.1 (giving the result that the PMEPR bound is $\frac{1}{n}(P_A + P_B)$) still holds, and we can use it to calculate the PMEPR bound for complementary QAM sequences.

5.2 Properties of Complementary QAM Sequences

5.2.1 Transforms that Preserve Complementarity

Phase Rotations

Let $\mathbf{a}'$ be the image of $\mathbf{a}$ after a phase rotation of angle θ. We note that $C_{\mathbf{a}}(u)$ is invariant under a phase rotation of any angle θ, since

$$C_{\mathbf{a}'}(u) = \sum_{0 \le i, i+u \le n-1} a_i e^{j\theta} a_{i+u}^* e^{-j\theta} = \sum_{0 \le i, i+u \le n-1} a_i a_{i+u}^* = C_{\mathbf{a}}(u).$$

Thus phase rotations do not affect complementarity. In particular, for the QAM constellations we are interested in, phase rotations of $\pi/2$, π, and $3\pi/2$ would map symbols in the constellation exactly onto another symbol in the same constellation.

Reflection

A complex number $|a|e^{j\angle a}$, when reflected in the line at an angle θ to the real axis passing through the origin, will be mapped onto the complex number $|a|e^{j(2\theta - \angle a)}$.

Let $\mathbf{a}'$ and $\mathbf{b}'$ be the images respectively of $\mathbf{a}$ and $\mathbf{b}$ after reflections in lines passing through the origin at angles α and β to the real axis respectively.

$$\begin{aligned} C_{\mathbf{a}'}(u) &= \sum_{0 \le i, i+u \le n-1} |a_i| e^{j(2\alpha - \angle a_i)} |a_{i+u}| e^{-j(2\alpha - \angle a_{i+u})} \\ &= \sum |a_i| e^{-j\angle a_i} |a_{i+u}| e^{j\angle a_{i+u}} \\ &= \sum a_i^* a_{i+u} = C_{\mathbf{a}}^*(u). \end{aligned}$$

Similarly, $C_{\mathbf{b}'}(u) = C^*_{\mathbf{b}}(u)$ is independent of the angle of reflection β. Thus,

$$C_{\mathbf{a}'}(u) + C_{\mathbf{b}'}(u) = C^*_{\mathbf{a}}(u) + C^*_{\mathbf{b}}(u) = [(P_A + P_B)\delta(u)]^* = (P_A + P_B)\delta(u),$$

since P_A, P_B and $\delta(u)$ are all real. Therefore, $\mathbf{a}'$ and $\mathbf{b}'$ form a pair of complementary sequences.

In particular, reflections into the line passing through the origin at an angle θ to the real axis, where θ is an integral multiple of $\pi/4$ will give mappings from a QAM constellation into the same QAM constellation.

We also note in passing that taking the conjugate of a sequence is a special case of reflection in the real axis.

Reversal

Let $\mathbf{a}'$ and $\mathbf{b}'$ be images of the sequences $\mathbf{a}$ and $\mathbf{b}$ with the symbol order reversed. Therefore, $\mathbf{a}' = (a_{n-1}a_{n-2}\ldots a_0)$ and $\mathbf{b}' = (b_{n-1}b_{n-2}\ldots b_0)$.

Now,

$$\begin{aligned} C_{\mathbf{a}'}(u) &= \sum_{0\le i,i+u\le n-1} a_i^{'} a_{i+u}^{'*} = \sum_{0\le i,i+u\le n-1} a_{n-i}a^*_{n-(i+u)} \\ &= \sum_{0\le i,i+u\le n-1} a_i^* a_{i+u} = C^*_{\mathbf{a}}(u). \end{aligned}$$

Using the same argument as in the case of reflection, $\mathbf{a}'$ is a complementary sequence. Furthermore, we find that the reflected image and the reversed image of a complementary sequence share the same autocorrelation function, which is the complex conjugate of the autocorrelation function of the original sequence.

Moreover, we note that the combined operations of reflection *and* reversal gives us a sequence which has the same autocorrelation function as the original sequence.

Symbol-wise Multiplication with Rows of a DFT-like Matrix

Consider the n by n discrete Fourier transform (DFT) matrix:

$$\begin{bmatrix} 1 & 1 & 1 & \cdots & 1 \\ 1 & \omega & \omega^2 & \cdots & \omega^{n-1} \\ 1 & \omega^2 & \omega^4 & \cdots & \omega^{2(n-1)} \\ 1 & \omega^3 & \omega^6 & \cdots & \omega^{3(n-1)} \\ \vdots & \vdots & \vdots & \ddots & \vdots \\ 1 & \omega^{n-1} & \omega^{2(n-1)} & \cdots & \omega^{(n-1)^2} \end{bmatrix}.$$

Let $\mathbf{a}'$ and $\mathbf{b}'$ be the symbol-wise multiplication of sequences $\mathbf{a}$ and $\mathbf{b}$ with the rth row of the above DFT matrix. Therefore, $A' = (a_1 \ a_2\omega^r \ a_3\omega^{2r} \ \ldots \ a_n\omega^{(n-1)r})$ and $B' = (b_1 \ b_2\omega^r \ b_3\omega^{2r} \ \ldots \ b_n\omega^{(n-1)r})$.

Now,

$$C_{\mathbf{a}'}(u) = \sum_{0 \le i, i+u \le n-1} a_i\omega^{(i-1)r} a^*_{i+u}\omega^{-(i+u-1)r} = \sum a_i a^*_{i+u}\omega^{-ur} = \omega^{-ur} C_{\mathbf{a}}(u).$$

Similarly,

$$C_{\mathbf{b}'}(u) = \omega^{-ur} C_{\mathbf{b}}(u).$$

Therefore,

$$\begin{aligned} C_{\mathbf{a}'}(u) + C_{\mathbf{b}'}(u) &= \omega^{-ur}[C_{\mathbf{a}}(u) + C_{\mathbf{b}}(u)] \\ &= (P_A + P_B)\delta(u). \end{aligned}$$

since $\omega^{-0} = 1$.

We thus conclude that $\mathbf{a}'$ and $\mathbf{b}'$ form a complementary pair.

Note that we did not make use of the DFT matrix constraint that $\omega = e^{j\frac{2\pi p}{n}}$, a primitive nth root of unity, p being any integer relatively prime to n. In fact, for our purposes, we do not want to have this unnecessary constraint on ω. Instead, we only wish to have $\omega = e^{\pi/2}$, e^{π} or $e^{3\pi/2}$ for the symbol-wise multiplication to yield a mapping to the same QAM constellation.

The idea of using a DFT-like matrix to generate complementary sequences might be potentially useful in the encoding and decoding of QAM codes employing complementary sequences.

We note that in the special case of $\omega = e^{\pi} = -1$ and choosing r odd, the transform is

equivalent to negating all the elements of even order in the sequence, a transform which Golay [3] showed also preserves complementarity in the binary (BPSK) case.

5.2.2 Length Extension of Complementary Sequences

Length Doubling by Concatenation

Let $\mathbf{s}_1 = (\mathbf{a}\ \mathbf{b}) = (a_0\ a_1\ \cdots\ a_{n-1}\ b_0\ b_1\ \cdots\ b_{n-1})$, $\mathbf{s}_2 = (\mathbf{a}\ -\mathbf{b}) = (a_0\ a_1\ \cdots\ a_{n-1}\ -b_0\ -b_1\ \cdots\ -b_{n-1})$.

$$\begin{aligned} C_{\mathbf{s}_1}(u) &= \sum_{0\le i,i+u\le n-1} a_i a_{i+u}^* + \sum_{0\le i,i+u\le n-1} b_i b_{i+u}^* + \sum_{i=n-u}^{n-1} a_i b_{i+u-n}^* \\ &= (P_A+P_B)\delta(u) + \sum_{i=n-u}^{n-1} a_i b_{i+u-n}^* \\ C_{\mathbf{s}_2}(u) &= \sum_{0\le i,i+u\le n-1} a_i a_{i+u}^* + \sum_{0\le i,i+u\le n-1} b_i b_{i+u}^* + \sum_{i=n-u}^{n-1} a_i \left(-b_{i+u-n}^*\right) \\ &= (P_A+P_B)\delta(u) - \sum_{i=n-u}^{n-1} a_i b_{i+u-n}^* \end{aligned}$$

Therefore,

$$C_{\mathbf{s}_1}(u) + C_{\mathbf{s}_2}(u) = 2(P_A+P_B)\delta(u)$$

and $\mathbf{s}_1$ and $\mathbf{s}_2$ are complementary pairs.

Length Doubling by Interleaving

Let $\mathbf{t}_1 = (a_0\ b_0\ a_1\ b_1\ \cdots\ a_{n-1}\ b_{n-1})$, and $\mathbf{t}_2 = (a_0\ -b_0\ a_1\ -b_1\ \cdots\ a_{n-1}\ -b_{n-1})$.

For odd u, $C_{\mathbf{t}_1}(u) = \sum a_i b_j$ for some set of pairs (i,j). And $C_{\mathbf{t}_2}(u) = \sum a_i(-b_j)$ for the same set of pairs (i,j). Therefore $C_{\mathbf{t}_1}(u) + C_{\mathbf{t}_2}(u) = 0$, for odd u.

For even u, we let $u = 2k$, where k is a positive integer. $C_{\mathbf{t}_1}(u) = C_{\mathbf{a}}(k) + C_{\mathbf{b}}(k) = (P_A+P_B)\delta(u)$, and $C_{\mathbf{t}_2}(u) = C_{\mathbf{a}}(k) + C_{\mathbf{b}}(k) = (P_A+P_B)\delta(u)$. Therefore

$$C_{\mathbf{t}_1}(u) + C_{\mathbf{t}_2}(u) = 2(P_A+P_B)\delta(u).$$

$\mathbf{t}_1$ and $\mathbf{t}_2$ are thus complementary pairs.

Synthesis using QPSK Complementary Sequences

Suppose we have a pair of length n QAM complementary sequences $\mathbf{a}$ and $\mathbf{b}$, and a pair of length m QPSK complementary sequences $\mathbf{c}$ and $\mathbf{d}$. By QPSK, we refer to the signal

constellation where the possible symbols are 1, j, -1, and $-j$.

Consider the sequences of length $2mn$: $\mathbf{u}_1 = (c_0\mathbf{a}\ \ c_1\mathbf{a}\ \cdots\ c_{m-1}\mathbf{a}\ \ d_0\mathbf{b}\ \ d_1\mathbf{b}\ \cdots\ d_{m-1}\mathbf{b})$ and $\mathbf{u}_2 = (d^*_{m-1}\mathbf{a}\ \ d^*_{m-2}\mathbf{a}\ \cdots\ d^*_0\mathbf{a}\ \ -c^*_{m-1}\mathbf{b}\ \ -c^*_{m-2}\mathbf{b}\ \cdots\ -c^*_0\mathbf{b})$.

$C_{\mathbf{u}_1}(u)$ can be treated as the sum of three types of products. First, the product of two terms within the same subseries (e.g. $c_1\mathbf{a}$). We shall denote the sum of all such products as $C^1_{\mathbf{u}_i}(u)$. Second, the product of terms not in the same subseries, but both coming from $\mathbf{a}$, or from $\mathbf{b}$ (e.g. c_1a_2 and c_2a_5). We shall denote the sum of all such products as $C^2_{\mathbf{u}_i}(u)$. Third, the product of one term from an $\mathbf{a}$ sequence, and one term from a $\mathbf{b}$ sequence. We shall denote the sum of all such products as $C^3_{\mathbf{u}_i}(u)$. We will consider each type separately.

For the sum of products made up of two symbols within the same subseries,

$$\begin{aligned}
C^1_{\mathbf{u}_1}(u) &= \sum_{k=0}^{m-1} \sum_{0\le i,i+u\le n-1} c_k a_i c^*_k a^*_{i+u} + \sum_{l=0}^{m-1} \sum_{0\le i,i+u\le n-1} d_l b_i d^*_l b^*_{i+u} \\
&= \sum_{k=0}^{m-1} \sum_{0\le i,i+u\le n-1} a_i a^*_{i+u} + \sum_{l=0}^{m-1} \sum_{0\le i,i+u\le n-1} b_i b^*_{i+u} \\
&= mC_{\mathbf{a}}(u) + mC_{\mathbf{b}}(u) = m(P_A+P_B)\delta(u) \\
C^1_{\mathbf{u}_2}(u) &= \sum_{k=m-1}^{0} \sum_{0\le i,i+u\le n-1} d^*_k a_i d_k a^*_{i+u} + \sum_{l=m-1}^{0} \sum_{0\le i,i+u\le n-1} (-c^*_l) b_i (-c_l) b^*_{i+u} \\
&= \sum_{k=0}^{m-1} \sum_{0\le i,i+u\le n-1} a_i a^*_{i+u} + \sum_{l=0}^{m-1} \sum_{0\le i,i+u\le n-1} b_i b^*_{i+u} \\
&= mC_{\mathbf{a}}(u) + mC_{\mathbf{b}}(u) = m(P_A+P_B)\delta(u)
\end{aligned}$$

since $c_kc^*_k = 1$ and $d_ld^*_l = 1$. Therefore,

$$C^1_{\mathbf{u}_1}(u) + C^1_{\mathbf{u}_2}(u) = 2m(P_A+P_B)\delta(u).$$

For the sum of products of two symbols from different subseries but coming from the same sequence $\mathbf{a}$ or $\mathbf{b}$, when calculating $C^2_{\mathbf{u}_1}(u)$, consider the partial sum which contains only products in which the first term is derived from the ith term of sequence $\mathbf{a}$. Letting $u = vn + w$, where $w = u \bmod n$, this partial sum is either

$$\sum_{0\le k,k+v\le m-1} c_k a_i c^*_{k+v} a^*_{i+w} = \left(a_i a^*_{i+w}\right) \sum_{0\le k,k+v\le m-1} c_k c^*_{k+v}$$

for $i + w < n$, or

$$\sum_{0\le k,k+v+1\le m-1} c_k a_i c^*_{k+v+1} a^*_{i+w-n} = \left(a_i a^*_{i+w-n}\right) \sum_{0\le k,k+v+1\le m-1} c_k c^*_{k+v+1}$$

for $i + w \ge n$.

In either case, there is a corresponding partial sum for $C^2_{\mathbf{u}_2}(u)$ which is either

$$\sum_{0\le k,k+v\le m-1} d^*_{m-1-k}a_i d_{m-1-(k+v)}a^*_{i+w} = \left(a_i a^*_{i+w-n}\right)\sum_{0\le k,k+v\le m-1} d_k d^*_{k+v}$$

for $i+w<n$, or

$$\sum_{0\le k,k+v+1\le m-1} d^*_{m-1-k}a_i d_{m-1-(k+v+1)}a^*_{i+w-n} = \left(a_i a^*_{i+w-n}\right)\sum_{0\le k,k+v+1\le m-1} d_k d^*_{k+v+1}$$

for $i+w\ge n$, respectively.

The same applies for partial sums involving products in which the terms are derived from the sequence $\mathbf{b}$.

Combining the corresponding partial sums, we get for $i+w<n$

$$\begin{aligned}\left(a_i a^*_{i+w-n}\right)\sum_{0\le k,k+v\le m-1} c_k c^*_{k+v} &+ \left(a_i a^*_{i+w-n}\right)\sum_{0\le k,k+v\le m-1} d_k d^*_{k+v}\\ &= \left(a_i a^*_{i+w-n}\right)\left[C_{\mathbf{c}}(v)+C_{\mathbf{d}}(v)\right]\\ &= 0.\end{aligned}$$

since C and D are complementary and $v\neq 0$.

Similarly for $i+w\ge n$,

$$\begin{aligned}\left(a_i a^*_{i+w-n}\right)\sum_{0\le k,k+v+1\le m-1} c_k c^*_{k+v+1} &+ \left(a_i a^*_{i+w-n}\right)\sum_{0\le k,k+v+1\le m-1} d_k d^*_{k+v+1}\\ &= \left(a_i a^*_{i+w-n}\right)\left[C_{\mathbf{c}}(v+1)+C_{\mathbf{d}}(v+1)\right]\\ &= 0.\end{aligned}$$

Therefore, the total sum $C^2_{\mathbf{u}_1}(u)+C^2_{\mathbf{u}_2}(u)$ must equal to zero since the partial sums are all equal to zero.

For the sum $C^3_{\mathbf{u}_i}(u)$, where the terms in the sum are the products of one term from an $\mathbf{a}$ sequence, and one term from a $\mathbf{b}$ sequence, let us first consider a specific term in $C^3_{\mathbf{u}_1}(u)$, $c_i a_j d^*_k b^*_l$, where $0\le i,k\le m-1$, $0\le j,l\le n-1$. The distance v_1 between the symbols $c_i a_j$ and $d_k b_l$ in sequence $\mathbf{u}_1$ is $m(m+k)+l-[mi+j]=m^2+m(k-i)+(l-j)$.

Now consider the corresponding term in $C^3_{\mathbf{u}_2}(u)$, $-d^*_k a_j c_i b^*_l$, which is the negative of the term above. The distance v_2 between the symbols $d^*_k a_j$ and $-c^*_i b_l$ in sequence $\mathbf{u}_2$ is $m(m+m-i)+l-[m(m-k)+j]=m^2+m(k-i)+l-j$ which is equal to v_1.

Letting $v=v_1=v_2$, we see that for every term in $C^3_{\mathbf{u}_1}(v)$, there is a unique corresponding

negative term in $C^3_{\mathbf{u}_2}(v)$. Therefore the sum $C^3_{\mathbf{u}_1}(v)+C^3_{\mathbf{u}_2}(v)$ must equal to zero. Now, since

$$\begin{aligned} C_{\mathbf{u}_1}(u) + C_{\mathbf{u}_2}(u) &= \left[C^1_{\mathbf{u}_1}(u) + C^2_{\mathbf{u}_1}(u) + C^3_{\mathbf{u}_1}(u)\right] + \left[C^1_{\mathbf{u}_2}(u) + C^2_{\mathbf{u}_2}(u) + C^3_{\mathbf{u}_2}(u)\right] \\ &= \left[C^1_{\mathbf{u}_1}(u) + C^1_{\mathbf{u}_2}(u)\right] + \left[C^2_{\mathbf{u}_1}(u) + C^2_{\mathbf{u}_2}(u)\right] + \left[C^3_{\mathbf{u}_1}(u) + C^3_{\mathbf{u}_2}(u)\right] \\ &= 2m(P_A + P_B)\delta(u) + 0 + 0 \\ &= 2m(P_A + P_B)\delta(u), \end{aligned}$$

$\mathbf{u}_1$ and $\mathbf{u}_2$ are complementary sequences of length $2mn$.

By following a proof very similar to the one presented above, we can show that the interleaved sequences of length $2mn$ (formed from $\mathbf{a}$, $\mathbf{b}$, $\mathbf{c}$, and $\mathbf{d}$ as above):

$$\mathbf{v}_1 = (c_0\mathbf{a} \;\; d_0\mathbf{b} \;\; c_1\mathbf{a} \;\; d_1\mathbf{b} \;\; \cdots \;\; c_{m-1}\mathbf{a} \;\; d_{m-1}\mathbf{b})$$

and

$$\mathbf{v}_2 = (d^*_{m-1}\mathbf{a} \;\; -c^*_{m-1}\mathbf{b} \;\; d^*_{m-2}\mathbf{a} \;\; -c^*_{m-2}\mathbf{b} \;\; \cdots \;\; d^*_0\mathbf{a} \;\; -c^*_0\mathbf{b})$$

are also complementary.

The above properties of complementary QAM sequences, based in part on the rich reflective and rotational symmetries afforded by rectangular QAM constellations, strongly suggest the existence of code structures describing, if not all, at least a large subset of the set of complementary QAM sequences, just as Davis and Jedwab demonstrated with their result linking polyphase complementary sequences with Reed-Muller codes. The remaining sections in this chapter, representing the bulk of the original research performed for this thesis, will present and prove the constructions of 4-QAM, 16-QAM and 8-QAM sequences with low PMEPR, with code structures that allow for relatively simple encoding and decoding.

Although the properties shown in this section will not be used explicitly in the following sections, they were exploited extensively to simplify the computer searches performed to uncover the code structures in complementary QAM sequences.

5.3 Construction of 4-QAM Sequences with Low PMEPR

5.3.1 A Link Between BPSK and 4-QAM Constellations

We realize the BPSK constellation as the set

$$\text{BPSK} = \{\exp(j\pi x),\, x = 0, 1\} = \{+1, -1\}$$

and the 4-QAM constellation as the set

$$4\text{QAM} = \left\{\exp\left[j\left(\tfrac{\pi x}{2} + \tfrac{\pi}{4}\right)\right], x = 0, 1, 2, 3\right\}.$$

Let $\mathbb{Z}_2 = \{0, 1\}$, endowed with addition modulo 2. One can associate with any BPSK sequence $\mathbf{b} = b_0 b_1 \cdots b_{n-1}$ a unique sequence $\mathbf{x} = x_0 x_1 \cdots x_{n-1}$ where $x_i \in \mathbb{Z}_2$, $0 \leq i \leq n-1$ and $b_i = (-1)^{x_i}$. Throughout this work, we may occasionally denote $S_{\mathbf{b}}(t)$ and $P_{\mathbf{b}}(t)$ respectively by $S_{\mathbf{x}}(t)$ and $P_{\mathbf{x}}(t)$, when there is no ambiguity.

For any set of complex numbers $\mathcal{A}$, and any complex number a let $a\mathcal{A}$ denote the set $\{az \mid z \in \mathcal{A}\}$. If $\mathcal{A}$ and $\mathcal{B}$ are sets consisting of complex numbers then we define the set sum

$$\mathcal{A} + \mathcal{B} = \{z_1 + z_2 \mid z_1 \in \mathcal{A} \text{ and } \mathrm{z}_2 \in \mathcal{B}\}.$$

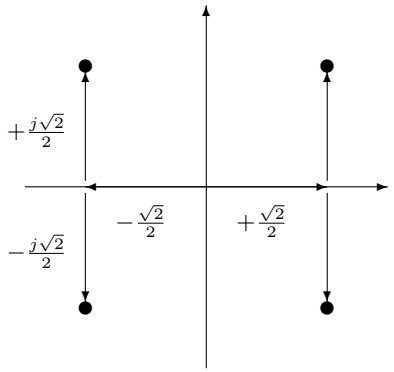

Figure 5-2: 4-QAM constellation as the 'sum' of two BPSK

It is easy to see from Figure 5-2 that

$$4\text{QAM} = \frac{\sqrt{2}}{2}\text{BPSK} + \frac{\sqrt{2}}{2} j \cdot \text{BPSK}. \tag{5.1}$$

Thus any point of the 4-QAM constellation can be written as

$$\frac{\sqrt{2}}{2}(-1)^x + \frac{\sqrt{2}}{2} j (-1)^y$$

for some $x, y \in \mathbb{Z}_2$. In this way one can associate with any 4-QAM sequence $\mathbf{c} = c_0 c_1 \cdots c_{n-1}$ a unique sequence $(x_0, y_0), (x_1, y_1), \cdots, (x_{n-1}, y_{n-1})$ where $(x_i, y_i) \in \mathbb{Z}_2 \times \mathbb{Z}_2$, $0 \leq i \leq n-1$. In particular, we may write

$$S_{\mathbf{x},\mathbf{y}}(t) := S_{\mathbf{c}}(t) = \frac{\sqrt{2}}{2} \sum_{i=0}^{n-1} ((-1)^{x_i} + j(-1)^{y_i}) \exp\left[2\pi j (f_0 + i\Delta f) t\right], \tag{5.2}$$

where $\mathbf{x} = x_0 x_1 \cdots x_{n-1}$ and $\mathbf{y} = y_0 y_1 \cdots y_{n-1}$.

Simplifying the above, the instantaneous envelope power is given by

$$P_{\mathbf{c}}(t) = P_{\mathbf{x},\mathbf{y}}(t) := |S_{\mathbf{x},\mathbf{y}}(t)|^2 = \frac{1}{2}\left|\sum_{i=0}^{n-1}((-1)^{x_i} + j(-1)^{y_i})\exp(2\pi ji\Delta ft)\right|^2.$$

In other words

$$P_{\mathbf{x},\mathbf{y}}(t) = \frac{1}{2}\,|\,S_{\mathbf{x}}(t) + jS_{\mathbf{y}}(t)|^2. \tag{5.3}$$

5.3.2 Construction of 4-QAM Codes from BPSK Codes

The observations made above leads us to consider the following construction:

Construction: Let $\mathcal{C}_1$ and $\mathcal{C}_2$ denote BPSK codes of length n. Then the codewords of $\mathcal{C}_1$ and $\mathcal{C}_2$ may be thought of as complex vectors of length n. The set sum

$$\mathcal{C} = \frac{\sqrt{2}}{2}\mathcal{C}_1 + \frac{\sqrt{2}}{2}j\cdot\mathcal{C}_2,$$

is the 4-QAM *code sum* of $\mathcal{C}_1$ and $\mathcal{C}_2$.

Clearly, the codewords of $\mathcal{C}$ are defined over the 4-QAM constellation. Moreover if $\mathcal{C}_1$ and $\mathcal{C}_2$ have respectively N_1 and N_2 codewords, then $\mathcal{C}$ has N_1N_2 codewords.

We now prove a simple Lemma.

Lemma 5.1 *Let $\mathcal{C}_1$ and $\mathcal{C}_2$ denote BPSK codes. Suppose that* $\mathrm{PMEPR}(\mathbf{c}_1) \le B_1$ *and* $\mathrm{PMEPR}(\mathbf{c}_2) \le B_2$ *for all $\mathbf{c}_1 \in \mathcal{C}_1$ and $\mathbf{c}_2 \in \mathcal{C}_2$, then* $\mathrm{PMEPR}(\mathbf{c}) \le \frac{1}{2}(\sqrt{B_1} + \sqrt{B_2})^2$ *for all $\mathbf{c} \in \mathcal{C}$.*

Proof: Let $\mathbf{c} = \frac{\sqrt{2}}{2}(\mathbf{c}_1 + j\mathbf{c}_2)$. Using Equation (5.3), we observe that

$$P_{\mathbf{c}}(t) = \tfrac{1}{2}\,|S_{\mathbf{c}_1}(t) + jS_{\mathbf{c}_2}(t)|^2.$$

By the triangle inequality we have

$$|S_{\mathbf{c}_1}(t) + jS_{\mathbf{c}_2}(t)| \le |S_{\mathbf{c}_1}(t)| + |jS_{\mathbf{c}_2}(t)| = |S_{\mathbf{c}_1}(t)| + |S_{\mathbf{c}_2}(t)|.$$

By assumption

$$\mathrm{PMEPR}(\mathbf{c}_i) = \tfrac{|S_{\mathbf{c}_i}(t)|^2}{n} \le B_i,$$

for $i = 1, 2$. Thus

$$|S_{\mathbf{c}_1}(t)| \le \sqrt{B_1 n}, \qquad |S_{\mathbf{c}_2}(t)| \le \sqrt{B_2 n}.$$

Combining these inequalities

$$P_{\mathbf{c}}(t) \le \tfrac{n}{2}(\sqrt{B_1} + \sqrt{B_2})^2.$$

Thus $\mathrm{PMEPR}(\mathbf{c}) \le \frac{1}{2}(\sqrt{B_1} + \sqrt{B_2})^2$. □

5.3.3 Construction of Sequences with PMEPR ≤ 4

Recalling the theorem of Davis and Jedwab [1] proved in section 4.2.2, in particular for the binary ($h = 1$) case,

Theorem 5.2 *Let π denote any permutation of the set $1, 2, \cdots, m$. Then any element $\mathbf{c}$ of $g(RM(1,m) + \sum_{k=1}^{m-1} x_{\pi(k)}x_{\pi(k+1)})$ is a BPSK vector of length 2^m with PMEPR$(\mathbf{c}) \leq 2$.*

The above result gives $m!/2$ cosets of the first order Reed-Muller code $RM(1,m)$ in the second order Reed-Muller code $RM(2,m)$. The images of the codewords of each coset have PMEPR ≤ 2.

Our construction is summarized by the following theorem.

Theorem 5.3 *Let π_1, π_2 denote any two permutations of the set $1, 2, \cdots, m$. For $l = 1, 2$, let $\mathcal{C}_l = g(RM(1,m) + \sum_{i=1}^{m-1} x_{\pi_l(i)}x_{\pi_l(i+1)})$. Then any element $\mathbf{c}$ of*

$$\frac{\sqrt{2}}{2}\mathcal{C}_1 + \frac{\sqrt{2}}{2}j\mathcal{C}_2 \tag{5.4}$$

is a 4-QAM vector of length 2^m with PMEPR$(\mathbf{c}) \leq 4$.

Proof: The result follows immediately from Theorem 5.2 and Lemma 5.1. □

The above result thus produces $(\frac{m!}{2})^2 4^{m+1}$ sequences that have PMEPR ≤ 6 dB. It is easy to see that these sequences are new as they are not covered by the theorems of [1] and [4]. In the next section, we establish that these sequences are amenable to a very simple maximum likelihood OFDM decoding algorithm. In this light, they are useful for practical applications.

5.3.4 ML OFDM Decoding Algorithm for Constructed Code

In order to provide an ML OFDM decoding algorithm for the sequences constructed above, we will link the ML OFDM decoding algorithm to the minimum distance algorithm.

To this end, let $\mathcal{C}$ denote any code defined over an equal energy constellation (such as BPSK, QPSK, and 8-PSK). Consider the OFDM transmission model given in Chapter 2 where the transmission employs codewords of $\mathcal{C}$. If the channel gains are $\alpha_i, i = 0, 1, \cdots, n-1$, the ML decoder decides in favor of the codeword $\mathbf{c} = c_0 c_1 \ldots c_{n-1}$ if it minimizes the decision metric

$$\sum_{i=0}^{n-1} |r_i - \alpha_i c_i|^2 \tag{5.5}$$

amongst all possible codewords.

Next, we expand

$$\sum_{i=0}^{n-1} |r_i - \alpha_i c_i|^2 = \sum_{i=0}^{n-1} (r_i r_i^* + |\alpha_i|^2 |c_i|^2) - \sum_{i=0}^{n-1} (r_i \alpha_i^* c_i^* + r_i^* \alpha_i c_i).$$

The first part of the sum does not depend on the codeword because all the constellation elements have equal energy. Thus the ML OFDM decoder decides in favor of the codeword $\mathbf{c} = c_0 c_1 \dots c_{n-1}$ if it minimizes the decision metric

$$-\sum_{i=0}^{n-1} (r_i \alpha_i^* c_i^* + r_i^* \alpha_i c_i). \tag{5.6}$$

Next, we add $\sum_{i=0}^{n-1} (|r_i|^2 |\alpha_i|^2 + |c_i|^2)$–which is again a constant independent of the codewords– to the above sum. We conclude that the ML OFDM decoder decides in favor of the codeword $\mathbf{c} = c_0 c_1 \dots c_{n-1}$, if it minimizes the decision metric

$$\sum_{i=0}^{n-1} (|r_i|^2 |\alpha_i|^2 + |c_i|^2) - \sum_{i=0}^{n-1} (r_i \alpha_i^* c_i^* + r_i^* \alpha_i c_i).$$

which in turn is equal to

$$\sum_{i=0}^{n-1} |r_i \alpha_i^* - c_i|^2. \tag{5.7}$$

Summarizing the above, we arrive at the following simple albeit fundamental Lemma.

Lemma 5.4 *With the notation as above, if the OFDM code is defined over an equal energy constellation, then the ML OFDM decoder is the output of the minimum distance decoder for $\mathcal{C}$ upon the input $(r_0 \alpha_0^*, \cdots, r_{n-1} \alpha_{n-1}^*)$.*

Next, we have another important Lemma.

Lemma 5.5 *Let $\mathcal{C}_1$ and $\mathcal{C}_2$ denote BPSK codes of length n and let*

$$\mathcal{C} = \frac{\sqrt{2}}{2} \mathcal{C}_1 + \frac{\sqrt{2}}{2} j \mathcal{C}_2,$$

denote the 4-QAM code sum of $\mathcal{C}_1$ and $\mathcal{C}_2$. Suppose that $R^1 = (r_0^1, r_1^1, \cdots, r_{n-1}^1)$ and $R^2 = (r_0^2, r_1^2, \cdots, r_{n-1}^2)$ are two arbitrary n-dimensional real vectors. Suppose that $\mathbf{c}_1$ and $\mathbf{c}_2$ are respectively the closest codewords of $\mathcal{C}_1$ to $\sqrt{2} R^1$ and $\mathcal{C}_2$ to $\sqrt{2} R^2$. Then $\frac{\sqrt{2}}{2} \mathbf{c}_1 + \frac{\sqrt{2}}{2} j \mathbf{c}_2$ is the closest point of $\mathcal{C}$ to $R^1 + j R^2$.

Proof: Clearly

$$|R^1 + j R^2 - (\frac{\sqrt{2}}{2} \mathbf{c}_1 + \frac{\sqrt{2}}{2} j \mathbf{c}_2)|^2 = \frac{1}{2} \left(|\sqrt{2} R^1 - \mathbf{c}_1|^2 + |\sqrt{2} R^2 - \mathbf{c}_2|^2 \right).$$

Thus to minimize the left side of the above equality $\mathbf{c}_1$ and $\mathbf{c}_2$ must be the closest codewords of $\mathcal{C}_1$ to $\sqrt{2}R^1$ and $\mathcal{C}_2$ to $\sqrt{2}R^2$. $\square$

We now proceed to present our decoder for the codes presented in the previous section. As in Theorem 5.3, let π_1, π_2 denote permutations of the set $0, 1, \cdots, m-1$ and for $l = 1, 2$, let $\mathcal{C}_l = g(RM(1,m) + \sum_{k=1}^{m-1} x_{\pi_l(k)} x_{\pi_l(k+1)})$. By Lemmas 5.4 and 5.5, in order to present an ML OFDM decoding algorithm for $\mathcal{C} = \frac{\sqrt{2}}{2}\mathcal{C}_1 + \frac{\sqrt{2}}{2} j\mathcal{C}_2$, it suffices to present a minimum distance decoding algorithm for $\mathcal{C}_l$, $l = 1, 2$ for any real vector $(r_0, r_1, \cdots, r_{2^m-1})$. We provide such a minimum distance algorithm for $g(RM(1,m) + \mathbf{f})$ where $\mathbf{f} = (f_0, f_1, \cdots, f_{2^m-1})$ is any arbitrary binary vector of length 2^m.

Let $R = ((-1)^{f_0} r_0, (-1)^{f_1} r_1, \cdots, (-1)^{f_{n-1}} r_{n-1})$. It is easy to see that determining the closest codeword of $g(RM(1,m) + \mathbf{f})$ to $(r_0, r_1, \cdots, r_{2^m-1})$ is equivalent to determining the closest codeword of $g(RM(1,m))$ to R. Thus, we provide an algorithm for the latter task.

To this end, let $O(m)$ denote the set of Boolean functions generated by $x_0, x_1, \cdots, x_{m-1}$, then $RM(1,m) = O(m) \cup (O(m) + 1)$. The image of $O(m)$ under $g(\cdot)$ is a set of 2^m orthogonal vectors with elements ± 1. Thus, the elements of $g(O(m))$ can be viewed as the rows of a Hadamard matrix H_{2^m}. The elements of $g(O(m) + 1)$ are then the rows of matrix $-H_{2^m}$. To find the closest row of $\pm H_{2^m}$ to the real vector R is equivalent to finding the element with the the largest absolute value in $H_{2^m} R^T$ (the Hadamard transform of R^T), where R^T is the transpose of R. If for some $0 \leq k \leq 2^m - 1$, the k-th element y_k of the vector $(y_0, y_1, \cdots, y_{2^m-1})^T = H_{2^m} R^T$ has the largest absolute value amongst all $y_l, l = 0, 1, 2 \cdots, 2^m - 1$, then the closest codeword of $g(RM(1,m))$ to R is the k-th row of H_{2^m} or $-H_{2^m}$ depending on whether the sign of y_k is positive or negative respectively. Thus, it suffices to compute $H_{2^m} R^T$. For this computational task, because of the recursive structure of Reed-Muller codes algorithms based on the Fast Hadamard Transform which are well-known in the art, the complexity of such a computation can be easily shown to be $m2^m$ real additions and subtractions.

Note that the decoding is extremely simple in the case when only one $\mathbf{f}$ each is used for the BPSK components of the 4-QAM sequence. However, complexity increases as we increase the code rate by making use of more possibilities for $\mathbf{f}$. At the highest rate, i.e. when we make use of all $(m!/2)^2 4^{m+1}$ codewords, each constituent BPSK code consists of $m!/2$ cosets of RM$(1,m)$, and therefore $m!/2$ applications of the FHT are needed for each component of the sum, making a total of $m!$ FHTs. This is still reasonably efficient

for small m, but not necessarily so for large m.

5.4 Construction of Complementary 16-QAM Sequences from 4-QAM Sequences

Rößing[5] and a to-be-published paper by Rößing and Tarokh[6] demonstrated a construction of 16-QAM sequences from 4-QAM Golay complementary sequences, and derived bounds for the PMEPR of the 16-QAM sequences.

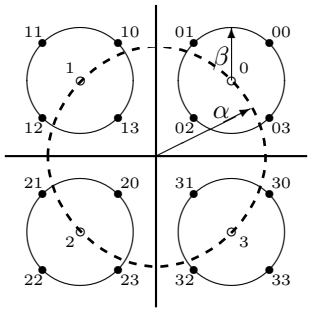

Figure 5-3: Constructing 16-QAM symbols from two 4-QAM symbols

Using the definition of the set sum as in section 5.3.1, we observe from figure 5-3 that

$$16\text{QAM} = \alpha(4\text{QAM}) + \beta(4\text{QAM}). \tag{5.8}$$

When the *major radius* $\alpha = \frac{2}{\sqrt{5}}$ and the *minor radius* $\beta = \frac{1}{\sqrt{5}}$, 16QAM, and 4QAM refer to the 16-QAM and 4-QAM constellations normalized to have unit average energy. Thus any point on the 16-QAM constellation can be written as

$$\frac{2}{\sqrt{5}} \exp\left(\frac{\pi j}{4}\right) j^x + \frac{1}{\sqrt{5}} \exp\left(\frac{\pi j}{4}\right) j^y$$

for some $x, y \in \mathbb{Z}_4$. In this way one can associate with any 16-QAM sequence $\mathbf{c} = c_0 c_1 \cdots c_{n-1}$ a unique sequence $(x_0, y_0), (x_1, y_1), \cdots, (x_{n-1}, y_{n-1})$ where $(x_i, y_i) \in \mathbb{Z}_4 \times \mathbb{Z}_4$, $0 \leq i \leq n-1$. In particular, we may write

$$S_{\mathbf{x},\mathbf{y}}(t) := S_{\mathbf{c}}(t) = \sum_{i=0}^{n-1} \left(\frac{2}{\sqrt{5}} j^{x_i} + \frac{1}{\sqrt{5}} j^{y_i}\right) \exp\left[2\pi j(f_0 + i\Delta f)t + \frac{\pi j}{4}\right], \tag{5.9}$$

where $\mathbf{x} = x_0 x_1 \cdots x_{n-1}$ and $\mathbf{y} = y_0 y_1 \cdots y_{n-1}$.

Simplifying the above, the instantaneous envelope power is given by

$$P_{\mathbf{x},\mathbf{y}}(t) := |S_{\mathbf{x},\mathbf{y}}(t)|^2 = \left| \sum_{i=0}^{n-1} \left(\frac{2}{\sqrt{5}} j^{x_i} + \frac{1}{\sqrt{5}} j^{y_i} \right) \exp\left(2\pi j i \Delta f t\right) \right|^2 .$$

In other words,

$$P_{\mathbf{x},\mathbf{y}}(t) = \left| \frac{2}{\sqrt{5}} S_{\mathbf{x}}(t) + \frac{1}{\sqrt{5}} S_{\mathbf{y}}(t) \right|^2 . \tag{5.10}$$

Figure 5-3 shows a way of labelling the 16-QAM symbols based on the two 4-QAM symbols it is constructed from. The first coordinate of the 16-QAM symbol describes the quadrant the symbol is in, and we shall call it the major coordinate. The second coordinate of the symbol pinpoints the exact location of the symbol within the quadrant, and we shall call it the minor coordinate.

Rößing and Tarokh[6] proved the following lemma, which calculates the mean envelope power for a particular subset of all possible 16-QAM sequences.

Lemma 5.6 *Let $C \subseteq \mathbb{Z}_4^n$ be a set of sequences that is invariant under the mapping $\mathbf{y} \rightarrow \mathbf{y} + \mathbf{2}$. Then for any set $A \subseteq \mathbb{Z}_4^n$, a normalized 16-QAM OFDM transmission using an equiprobable set of codewords $A \times C$ (or $C \times A$) requires a mean envelope power $P_{av} = n$.*

Proof: Let $\mathbf{c}$ denote a codeword corresponding to the pair $(\mathbf{x}, \mathbf{y}) \in A \times C$. Let $\mathbf{d}$ be the codeword corresponding to the pair $(\mathbf{x}, \mathbf{y} + \mathbf{2}) \in A \times C$. Then it is easy to see that $\|\mathbf{c}\|^2 + \|\mathbf{d}\|^2 = 2n$. The result follows by letting $(\mathbf{x}, \mathbf{y})$ run over $A \times C$ and noticing that the mapping $(\mathbf{x}, \mathbf{y}) \rightarrow (\mathbf{x}, \mathbf{y} + \mathbf{2})$ is a one-to-one and onto mapping. □

Rößing and Tarokh[6] derived peak envelope power bounds for three classes of constructed 16-QAM sequences, which we will list here. Using the above lemma, we can calculate the mean envelope powers for the latter two classes (averaged over only those described sequences, and not all possible uncoded sequences). Letting $\mathbf{c}$ denote the 16-QAM sequence constructed from 4-QAM sequences $\mathbf{x}$ and $\mathbf{y}$,

(**I**) If $\mathbf{x}$ is a Golay sequence, and $\mathbf{y} = \mathbf{x} + \mathbf{2}$, then $P_{\mathbf{x},\mathbf{x}+\mathbf{2}}(t) \leq 0.4n$.

(**II**) If $\mathbf{x}$ and $\mathbf{y}$ form a Golay complementary pair then $P_{\mathbf{x},\mathbf{y}}(t) \leq 2n$, PMEPR($\mathbf{c}$) ≤ 2.0.

(**III**) If $\mathbf{x}$ and $\mathbf{y}$ are Golay sequences, which do not necessarily form a Golay complementary pair, then $P_{\mathbf{x},\mathbf{y}}(t) \leq 3.6n$, PMEPR($\mathbf{c}$) ≤ 3.6.

Although [6] proved the PMEPR bounds above, it did not attempt to prove the complementarity of the sequences constructed. In the next section, we will prove the complementarity of the second class of 16-QAM sequences described above. After that, we will present and prove a construction of 16-QAM complementary sequences from 4-QAM complementary sequences as described by Davis and Jedwab [1]. This construction yields a large set of complementary 16-QAM sequences, with different well-defined PMEPR bounds for various distinct subsets of the entire set.

5.5 16-QAM Complementary Sequences formed from one 4-QAM Complementary Pair

Let $\mathbf{a} = a_0\ a_1\ \cdots a_{n-1}$ and $\mathbf{b} = b_0\ b_1\ \cdots b_{n-1}$ be a Golay complementary pair in $\mathbb{Z}_4^n$. Since they are complementary, they satisfy

$$C_{\mathbf{a}}(u) + C_{\mathbf{b}}(u) = \sum_{0 \le i, i+u \le n-1} \left[\xi^{a_i - a_{i+u}} + \xi^{b_i - b_{i+u}} \right] = 2n\delta(u). \tag{5.11}$$

Now consider the constructed 16-QAM sequences, $\mathbf{s}$ and $\mathbf{t}$,

$$s_i = \alpha\gamma\xi^{a_i} + \beta\gamma\xi^{b_i} \quad \text{and} \quad t_i = -\alpha\gamma\xi^{b_i} + \beta\gamma\xi^{a_i}.$$

where α is the major radius of the construction, β is the minor radius (as depicted in figure 5-3) and γ equals $e^{\frac{j\pi}{4}}$. For a normalized rectangular 16-QAM signal constellation with unit mean energy (if all symbols are equiprobable), α and β take the values $\frac{2}{\sqrt{5}}$, and $\frac{1}{\sqrt{5}}$ respectively,

$$\begin{aligned} C_{\mathbf{s}}(u) &= \sum_{0 \le i, i+u \le n-1} \left(\alpha\gamma\xi^{a_i} + \beta\gamma\xi^{b_i} \right) \left(\alpha\gamma\xi^{a_{i+u}} + \beta\gamma\xi^{b_{i+u}} \right)^* \\ &= \sum \left[\alpha^2 \xi^{a_i - a_{i+u}} + \alpha\beta \left(\xi^{a_i - b_{i+u}} + \xi^{b_i - a_{i+u}} \right) + \beta^2 \xi^{b_i - b_{i+u}} \right]. \end{aligned} \tag{5.12}$$

Similarly,

$$C_{\mathbf{t}}(u) = \sum \left[\alpha^2 \xi^{b_i - b_{i+u}} - \alpha\beta \left(\xi^{a_i - b_{i+u}} + \xi^{b_i - a_{i+u}} \right) + \beta^2 \xi^{a_i - a_{i+u}} \right]. \tag{5.13}$$

Now,

$$\begin{aligned} C_{\mathbf{s}}(u) + C_{\mathbf{t}}(u) &= \sum \left[\alpha^2 \left(\xi^{a_i - a_{i+u}} + \xi^{b_i - b_{i+u}} \right) + 0 + \beta^2 \left(\xi^{b_i - b_{i+u}} + \xi^{a_i - a_{i+u}} \right) \right] \\ &= \left(\alpha^2 + \beta^2 \right) \left[C_{\mathbf{a}}(u) + C_{\mathbf{b}}(u) \right] \\ &= 2n \left(\alpha^2 + \beta^2 \right) \delta(u). \end{aligned} \tag{5.14}$$

Since the sum of the autocorrelation functions satisfies the complementarity property, we have thus proven that $\mathbf{s}$ and $\mathbf{t}$ form a 16-QAM Golay complementary pair.

Substituting $\alpha = \frac{2}{\sqrt{5}}$ and $\beta = \frac{1}{\sqrt{5}}$ into (5.14) , we get $C_{\mathbf{s}}(u) + C_{\mathbf{t}}(u) = 2n\delta(u)$, which gives the same bound for PMEPR of 2 as in [6].

5.6 16-QAM Complementary Sequences formed from 4-QAM Complementary Sequences as described by Davis and Jedwab

Using two 4-QAM sequences to construct a 16-QAM sequence as before, but limiting the 4-QAM Golay complementary sequences describing the major coordinates to those of the form

$$2\sum_{k=1}^{m-1} x_{\pi(k)}x_{\pi(k+1)} + \sum_{k=1}^{m} c_k x_k + \mathbf{c}$$

as described by Davis and Jedwab [1], we describe a class of 16-QAM complementary sequences which are easy to encode, and improve on the PMEPR bounds derived in [6].

5.6.1 Theorem

Each 16-QAM symbol can be described by two 4-QAM symbol coordinates. Let the first 4-QAM symbol which determines the quadrant of the 16-QAM symbol be denoted as the major coordinate. Let the other 4-QAM symbol be denoted as the minor coordinate.

Now, let the sequence of major coordinates of the 16-QAM sequence we construct be a sequence of the form

$$a_{\text{major}}(x_1, x_2, \cdots, x_m) = 2\sum_{k=1}^{m-1} x_{\pi(k)}x_{\pi(k+1)} + \sum_{k=1}^{m} c_k x_k + \mathbf{c}.$$

If the minor coordinates of the 16-QAM sequence are set to any of the following, the

resulting sequence will be a complementary 16-QAM sequence.

$$a_{\text{minor}}(x_1,\cdots,x_m) = a_{\text{major}}(x_1,\cdots,x_m) + \begin{cases} \mathbf{0} & \\ x_{\pi(1)} & \\ x_{\pi(m)} & \\ 2x_{\pi(1)} & \\ 2x_{\pi(m)} & \\ 3x_{\pi(1)} & \\ 3x_{\pi(m)} & \\ x_{\pi(w)} + 3x_{\pi(w+1)} & 1 \le w \le m-1 \\ 2x_{\pi(w)} + 2x_{\pi(w+1)} & 1 \le w \le m-1 \\ 3x_{\pi(w)} + x_{\pi(w+1)} & 1 \le w \le m-1 \\ \mathbf{1} & \\ \mathbf{1} + x_{\pi(1)} & \\ \mathbf{1} + x_{\pi(m)} & \\ \mathbf{1} + 3x_{\pi(1)} & \\ \mathbf{1} + 3x_{\pi(m)} & \\ \mathbf{1} + 2x_{\pi(w)} & 1 \le w \le m \\ \mathbf{1} + x_{\pi(w)} + x_{\pi(w+1)} & 1 \le w \le m-1 \\ \mathbf{1} + 3x_{\pi(w)} + 3x_{\pi(w+1)} & 1 \le w \le m-1 \end{cases}$$

Adding $\mathbf{2}$ to any of the above cases, effectively negating all the minor coordinates will also give minor sequences that would yield complementary 16-QAM sequences when combined with the major sequence $a_{\text{major}}(x_1, x_2, \cdots, x_m)$.

Counting the number of possibilities of minor sequences above (remembering to double for the addition of $\mathbf{2}$), we find that for each major sequence of length 2^m, there are $14+12m$ possible minor sequences. Since there are $(\frac{m!}{2})4^{m+1}$ possible major sequences, the total number of 16-QAM sequences we have described is $(14+12m)(\frac{m!}{2})4^{m+1}$.

5.6.2 Proof

Let the monomials that are added to $a_{\text{major}}(x_1, x_2, \cdots, x_m)$ to obtain $a_{\text{minor}}(x_1, x_2, \cdots, x_m)$, as listed above, be generally denoted by $s(x_1, x_2, \cdots, x_m)$. Let us first explain our notation and derive some basic expressions that we will use in the proofs below.

Let $(i_1, i_2, \cdots, i_m)$ be the binary representation of i, that is, $i = \sum_{k=1}^{m} i_k 2^{m-k}$. Let A_i and a_i denote the ith element in the sequences $a_{\text{major}}(x_1, x_2, \cdots, x_m)$ and $a_{\text{minor}}(x_1, x_2, \cdots, x_m)$ respectively in $\mathbb{Z}_4$. Therefore,

$$\begin{aligned} A_i &= 2\sum_{k=1}^{m-1} i_{\pi(k)} i_{\pi(k+1)} + \sum_{k=1}^{m} c_k i_k + c \qquad (5.15) \\ a_i &= 2\sum_{k=1}^{m-1} i_{\pi(k)} i_{\pi(k+1)} + \sum_{k=1}^{m} c_k i_k + c + i_s \\ &= A_i + i_s \qquad (5.16) \end{aligned}$$

where $i_s = s_0 + \sum_{k=1}^{m} s_k i_k$ for $s(x_1, x_2, \cdots, x_m) = s_0 \cdot \mathbf{1} + \sum_{k=1}^{m} s_k x_k$ as listed on the previous page. Now, let

$$\mathcal{A}_i = \alpha\gamma\xi^{A_i} + \beta\gamma\xi^{a_i} \qquad (5.17)$$

denote the ith element of the 16-QAM sequence $\mathcal{A}$ constructed from $a_{\text{major}}(x_1, x_2, \cdots, x_m)$ and $a_{\text{minor}}(x_1, x_2, \cdots, x_m)$, where α is the radius of the major 4-QAM component, β the radius of the minor 4-QAM component, $\gamma = e^{j\frac{\pi}{4}}$, and $\xi = e^{j\frac{\pi}{2}}$.

Letting either

$$\begin{aligned} b_{\text{major}}(x_1, x_2, \cdots, x_m) &= a_{\text{major}}(x_1, x_2, \cdots, x_m) + 2x_{\pi(1)} \qquad (5.18) \\ b_{\text{minor}}(x_1, x_2, \cdots, x_m) &= a_{\text{minor}}(x_1, x_2, \cdots, x_m) + 2x_{\pi(1)} \qquad (5.19) \end{aligned}$$

or

$$\begin{aligned} b_{\text{major}}(x_1, x_2, \cdots, x_m) &= a_{\text{major}}(x_1, x_2, \cdots, x_m) + 2x_{\pi(m)} \qquad (5.20) \\ b_{\text{minor}}(x_1, x_2, \cdots, x_m) &= a_{\text{minor}}(x_1, x_2, \cdots, x_m) + 2x_{\pi(m)}, \qquad (5.21) \end{aligned}$$

we will show that for

$$\mathcal{B}_i = \alpha\gamma\xi^{B_i} + \beta\gamma\xi^{b_i} \qquad (5.22)$$

where either

$$\begin{aligned} B_i &= 2\sum_{k=1}^{m-1} i_{\pi(k)} i_{\pi(k+1)} + \sum_{k=1}^{m} c_k i_k + c + 2i_{\pi(1)} \\ &= A_i + 2i_{\pi(1)} \qquad (5.23) \\ b_i &= 2\sum_{k=1}^{m-1} i_{\pi(k)} i_{\pi(k+1)} + \sum_{k=1}^{m} c_k i_k + c + i_s + 2i_{\pi(1)} \\ &= a_i + 2i_{\pi(1)} = A_i + i_s + 2i_{\pi(1)} \qquad (5.24) \end{aligned}$$

or

$$\begin{aligned} B_i &= 2\sum_{k=1}^{m-1} i_{\pi(k)} i_{\pi(k+1)} + \sum_{k=1}^{m} c_k i_k + c + 2i_{\pi(m)} \\ &= A_i + 2i_{\pi(m)} \end{aligned} \tag{5.25}$$

$$\begin{aligned} b_i &= 2\sum_{k=1}^{m-1} i_{\pi(k)} i_{\pi(k+1)} + \sum_{k=1}^{m} c_k i_k + c + i_s + 2i_{\pi(m)} \\ &= a_i + 2i_{\pi(m)} = A_i + i_s + 2i_{\pi(m)}, \end{aligned} \tag{5.26}$$

at least one of the above two possibilities for $\mathcal{B}$ is a complementary pair of $\mathcal{A}$.

Using the facts that α, β are real, and that $\gamma\gamma^* = 1$ (where γ^* denotes the complex conjugate of γ), the auto-correlation functions for $\mathcal{A}$ and $\mathcal{B}$ are

$$\begin{aligned} C_{\mathcal{A}}(u) &= \sum_{0\le i, i+u\le n-1} \left(\alpha\gamma\xi^{A_i} + \beta\gamma\xi^{a_i}\right)\left(\alpha\gamma\xi^{A_{i+u}} + \beta\gamma\xi^{a_{i+u}}\right)^* \\ &= \sum_{0\le i, i+u\le n-1} \left[\alpha^2\xi^{(A_i - A_{i+u})} + \beta^2\xi^{(a_i - a_{i+u})} + \alpha\beta\left(\xi^{(A_i - a_{i+u})} + \xi^{(a_i - A_{i+u})}\right)\right] \end{aligned} \tag{5.27}$$

Similarly, we obtain for $\mathcal{B}$,

$$C_{\mathcal{B}}(u) = \sum_{0\le i, i+u\le n-1} \left[\alpha^2\xi^{(B_i - B_{i+u})} + \beta^2\xi^{(b_i - b_{i+u})} + \alpha\beta\left(\xi^{(B_i - b_{i+u})} + \xi^{(b_i - B_{i+u})}\right)\right] \tag{5.28}$$

It has been proven by Davis and Jedwab [1] that the QPSK sequences $A = (A_0, A_1, \cdots, A_{n-1})$ and $B = (B_0, B_1, \cdots, B_{n-1})$ form a complementary pair. Furthermore, the QPSK sequences $a = (a_0, a_1, \cdots, a_{n-1})$ and $b = (b_0, b_1, \cdots, b_{n-1})$ also form a complementary pair. Therefore, for $u \neq 0$

$$C_A(u) + C_B(u) = \sum_{0\le i, i+u\le n-1} \left[\xi^{(A_i - A_{i+u})} + \xi^{(B_i - B_{i+u})}\right] = 0 \tag{5.29}$$

$$C_a(u) + C_b(u) = \sum_{0\le i, i+u\le n-1} \left[\xi^{(a_i - a_{i+u})} + \xi^{(b_i - b_{i+u})}\right] = 0 \tag{5.30}$$

Therefore, adding equations (5.28) and (5.28), and using (5.29) and (5.30), we obtain

$$C_{\mathcal{A}}(u) + C_{\mathcal{B}}(u) = \sum_{0\le i, i+u\le n-1} \alpha\beta\left[\xi^{(A_i - a_{i+u})} + \xi^{(a_i - A_{i+u})} + \xi^{(B_i - b_{i+u})} + \xi^{(b_i - B_{i+u})}\right]$$

Using relations (5.16), (5.23), (5.24), (5.25), and (5.26), and letting $\pi(1|m)$ denote either $\pi(1)$ or $\pi(m)$, taking only one identity throughout, we get

$$\sum_{0\le i, i+u\le n-1} \left[\xi^{(A_i - a_{i+u})} + \xi^{(a_i - A_{i+u})}\right] = \sum \left[\xi^{A_i - A_{i+u}}\xi^{-(i+u)_s} + \xi^{A_i - A_{i+u}}\xi^{i_s}\right]$$

$$
\begin{aligned}
& & = & \sum \left[\xi^{A_i - A_{i+u}} \left(\xi^{i_s} + \xi^{-(i+u)_s} \right) \right] \\
\sum_{0 \le i, i+u \le n-1} \left[\xi^{(B_i - b_{i+u})} + \xi^{(b_i - B_{i+u})} \right] & = & \sum \left[\xi^{B_i - B_{i+u}} \left(\xi^{i_s} + \xi^{-(i+u)_s} \right) \right] \\
& = & \sum \left[\xi^{A_i - A_{i+u}} \xi^{2i_{\pi(1|m)} - 2(i+u)_{\pi(1|m)}} \left(\xi^{i_s} + \xi^{-(i+u)_s} \right) \right].
\end{aligned}
$$

where $(i+u)_s = \sum_{k=1}^{m} s_k (i+u)_k + s_0$, and $(i+u)_1, (i+u)_2, \cdots, (i+u)_m$ is the binary representation of $(i+u)$.

Summing the above expressions, we derive the following expression

$$
\begin{aligned}
C_{\mathcal{A}}(u) + C_{\mathcal{B}}(u) &= \alpha\beta \sum_{0 \le i, i+u \le n-1} \left[\xi^{A_i - A_{i+u}} \left(1 + \xi^{2i_{\pi(1|m)} - 2(i+u)_{\pi(1|m)}} \right) \left(\xi^{i_s} + \xi^{-(i+u)_s} \right) \right] \\
&= \alpha\beta \sum \left\{ \xi^{A_i - A_{i+u}} \left[1 + (-1)^{i_{\pi(1|m)} - (i+u)_{\pi(1|m)}} \right] \left(\xi^{i_s} + \xi^{-(i+u)_s} \right) \right\} \quad (5.31)
\end{aligned}
$$

We will be using this expression for $C_{\mathcal{A}}(u) + C_{\mathcal{B}}(u)$ in the proofs below.

For the cases of $s(x_1, x_2, \cdots, x_m) = s_0 \cdot \mathbf{1}$, $s_0 = 0, 1, 2, 3$

For these cases, it is clear that $a_i = A_i + s_0$. Therefore,

$$
\begin{aligned}
\mathcal{A}_i &= \alpha\gamma\xi^{A_i} + \beta\gamma\xi^{a_i} = (\alpha + \beta\xi^{s_0})\,\gamma\xi^{A_i} \\
\mathcal{B}_i &= \alpha\gamma\xi^{B_i} + \beta\gamma\xi^{b_i} = (\alpha + \beta\xi^{s_0})\,\gamma\xi^{B_i}
\end{aligned}
$$

Since Davis and Jedwab [1] proved that the QPSK sequences $A = (A_0, A_1, \cdots, A_{n-1})$ and $B = (B_0, B_1, \cdots, B_{n-1})$ form a complementary pair, where $B_i = A_i + 2i_{\pi(1|m)}$, for $u \neq 0$

$$
C_A(u) + C_B(u) = \sum_{0 \le i, i+u \le n-1} \left[\xi^{(A_i - A_{i+u})} + \xi^{(B_i - B_{i+u})} \right] = 0
$$

Now,

$$
\begin{aligned}
C_{\mathcal{A}}(u) + C_{\mathcal{B}}(u) &= |\alpha + \beta\xi^{s_0}|^2 \sum_{0 \le i, i+u \le n-1} \left[\xi^{(A_i - A_{i+u})} + \xi^{(B_i - B_{i+u})} \right] \\
&= |\alpha + \beta\xi^{s_0}|^2 \left[C_A(u) + C_B(u) \right] = 0
\end{aligned}
$$

Therefore, the constructed sequence $\mathcal{A}$ must be complementary.

Alternatively, we can interpret this case graphically by observing from Figure 5-4 that only a subset of the 16-QAM constellation points are used for any one particular value of s_0. Therefore, the resulting 16-QAM sequences are simply either scaled versions of the complementary 4-QAM sequence, $a_{\text{major}}(x_1, x_2, \cdots, x_m)$, for $s_0 = 0, 2$, or scaled and rotated versions of the same complementary 4-QAM sequence for $s_0 = 1, 3$. Since scaled

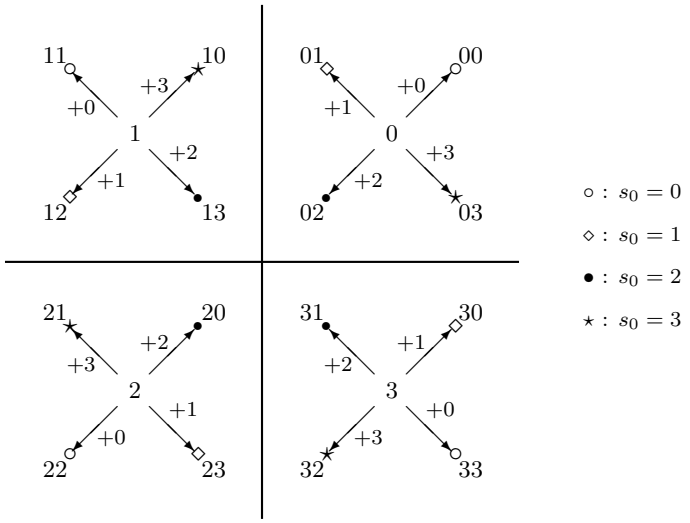

Figure 5-4: Subsets of 16-QAM constellation points used when $s_0 = 0, 1, 2, 3$

versions of complementary pairs continue to have the property that the sum of aperiodic correlations is zero, and correlations are invariant under rotation of the entire sequence, the resulting 16-QAM sequences are complementary.

For the cases of $s(x_1, x_2, \cdots, x_m) = x_{\pi(m)}, 2x_{\pi(m)}, 3x_{\pi(m)}, \mathbf{1} + x_{\pi(m)}, \mathbf{1} + 3x_{\pi(m)}$

For these cases, we will show that the complementary pair to $\mathcal{A}$ is $\mathcal{B}$ where $B_i = A_i + 2i_{\pi(1)}$, and $b_i = a_i + 2i_{\pi(1)}$.

We first note that (5.31) becomes

$$C_{\mathcal{A}}(u) + C_{\mathcal{B}}(u) \quad = \quad \alpha\beta \sum \left\{ \xi^{A_i - A_{i+u}} \left[1 + (-1)^{i_{\pi(1)} - (i+u)_{\pi(1)}} \right] \left(\xi^{i_s} + \xi^{-(i+u)_s} \right) \right\} \quad (5.32)$$

Table 5.1 shows the value of $\xi^{i_s} + \xi^{-(i+u)_s}$ for the various cases evaluated at all the possible combinations of $(i_{\pi(m)}, (i+u)_{\pi(m)})$.

We separate the terms in the sum (5.32) above into three non-overlapping types.

Type 1: Terms in which $i_{\pi(1)} \neq (i+u)_{\pi(1)}$

For terms of this type, the factor $\left[1 + (-1)^{i_{\pi(1)} - (i+u)_{\pi(1)}} \right]$ equals zero, therefore the sum of all terms of this type is zero.

Type 2: Terms in which $i_{\pi(1)} = (i+u)_{\pi(1)}$, and $\xi^{i_s} + \xi^{-(i+u)_s} = 0$

In this case, the third factor $\left(\xi^{i_{\pi(m)}} + \xi^{-(i+u)_{\pi(m)}} \right)$ equals zero, and so the sum of all terms of this type is also zero.

$i_{\pi(m)}$	$(i+u)_{\pi(m)}$	$\xi^{i_s}+\xi^{-(i+u)_s}$				
		$s=x_{\pi(m)}$	$s=2x_{\pi(m)}$	$s=3x_{\pi(m)}$	$s=\mathbf{1}+x_{\pi(m)}$	$s=\mathbf{1}+3x_{\pi(m)}$
0	0	2	2	2	0	0
0	1	$1-\xi$	0	$1+\xi$	$-1+\xi$	$1+\xi$
1	0	$1+\xi$	0	$1-\xi$	$-1-\xi$	$1-\xi$
1	1	0	-2	0	-2	2

Table 5.1: Values for the third factor $\xi^{i_s}+\xi^{-(i+u)_s}$ for cases $s(x_1,x_2,\cdots,x_m)=x_{\pi(m)}$, $2x_{\pi(m)}$, $3x_{\pi(m)}$, $\mathbf{1}+x_{\pi(m)}$, $\mathbf{1}+3x_{\pi(m)}$

Type 3: Terms in which $i_{\pi(1)}=(i+u)_{\pi(1)}$, and $\xi^{i_s}+\xi^{-(i+u)_s}\neq 0$

For terms of this type, the factor $\left[1+(-1)^{i_{\pi(1)}-(i+u)_{\pi(1)}}\right]$ equals 2, and $\left(\xi^{i_{\pi(m)}}+\xi^{-(i+u)_{\pi(m)}}\right)$ takes on values as shown in table 5.1.

Since we are only interested in calculating $C_{\mathcal{A}}(u)+C_{\mathcal{B}}(u)$ for $u\neq 0$, $i\neq i+u$. Now, let $j=i+u$. Define v to be the smallest integer for which $i_{\pi(v)}\neq j_{\pi(v)}$. By assumption, $v>1$ and by definition, $v\leq m$. Now, define i' and j' using their binary representations

$$i'=(i_1,i_2,\cdots,1-i_{\pi(v-1)},\cdots,i_m)\qquad\qquad j'=(j_1,j_2,\cdots,1-j_{\pi(v-1)},\cdots,j_m)$$

By assumption, $i_{\pi(v-1)}=j_{\pi(v-1)}$, and so $j'=i'+u$. We have, therefore, defined an invertible map from the ordered pair (i,j) to (i',j') and since $v-1$ cannot be equal to m, as $v\leq m$, $i_{\pi(m)}$ and $j_{\pi(m)}$ remain unchanged. Therefore both pairs would share the same value for the third factor $\xi^{i_s}+\xi^{-(i+u)_s}$. Hence in the sum $C_{\mathcal{A}}(u)+C_{\mathcal{B}}(u)$, terms corresponding to (i,j) and (i',j') have the same coefficients multiplying $\xi^{A_i-A_j}$ and $\xi^{A_{i'}-A_{j'}}$.

Substituting for i and i' in (5.15) gives

$$A_{i'}-A_i=2i_{\pi(v-2)}+2i_{\pi(v)}+c_{\pi(v-1)}-2c_{\pi(v-1)}i_{\pi(v-1)}$$

(unless $v=2$, in which case we just delete terms that involve $\pi(v-2)$ here and in what follows). Therefore,

$$\begin{aligned}A_i-A_j-A_{i'}+A_{j'} &= 2(j_{\pi(v-2)}-i_{\pi(v-2)})+2(j_{\pi(v)}-i_{\pi(v)})-2c_{\pi(v-1)}(j_{\pi(v-1)}-i_{\pi(v-1)})\\ &= \pm 2\end{aligned}$$

by the definition of v. Therefore,

$$\begin{aligned} \xi^{A_i - A_j - A_{i'} + A_{j'}} &= -1 \\ \xi^{A_i - A_j} &= -\xi^{A_{i'} - A_{j'}} \\ \xi^{A_i - A_j} + \xi^{A_{i'} - A_{j'}} &= 0 \end{aligned}$$

for each pair of (i, j) and (i', j'). Since in the sum the coefficient multiplying $\xi^{A_i - A_j}$ and $\xi^{A_{i'} - A_{j'}}$ are the same, the sum of all type 3 terms must also equal to zero.

Thus the sum of all three non-overlapping types of terms is zero, $C_{\mathcal{A}}(u) + C_{\mathcal{B}}(u) = 0$ for $u \neq 0$, and $\mathcal{A}$ and $\mathcal{B}$ are complementary 16-QAM sequences.

For the case of $s(x_1, x_2, \cdots, x_m) = 2x_{\pi(m)}$, an alternate proof would be to observe that a_i is actually complementary to A_i in this instance, as proved by Davis and Jedwab [1]. Thus the complementarity of $\mathcal{A}$ follows from the proof in section 5.5.

For the cases of $s(x_1, x_2, \cdots, x_m) = x_{\pi(1)}, 2x_{\pi(1)}, 3x_{\pi(1)}, \mathbf{1} + x_{\pi(1)}, \mathbf{1} + 3x_{\pi(1)}$

Consider the proof of the previous subsection. Now, if π is replaced by the permutation π' defined by $\pi'(k) = \pi(m + 1 - k)$ (reversal of the permutation), A_i is invariant, but a_i maps to $A_i + i_{\pi(1)}$, B_i maps to $A_i + 2i_{\pi(m)}$, and b_i maps to $a_i + 2i_{\pi(m)}$. Since we have already established the complementarity of $\mathcal{A}$ and $\mathcal{B}$ for the cases involving $x_{\pi(m)}$, this transformation shows us that letting $a_i = A_i + i_s$, where $s(x_1, x_2, \cdots, x_m) = x_{\pi(1)}$, $2x_{\pi(1)}$, $3x_{\pi(1)}$, $\mathbf{1} + x_{\pi(1)}$, or $\mathbf{1} + 3x_{\pi(1)}$, also yields complementary 16-QAM sequences, where the complementary pair is $\mathcal{B}$ where $B_i = A_i + 2i_{\pi(m)}$, $b_i = a_i + 2i_{\pi(m)}$.

For the case of $s(x_1, x_2, \cdots, x_m) = \mathbf{1} + 2x_{\pi(w)}$

For this case of $s(x_1, x_2, \cdots, x_m) = \mathbf{1} + 2x_{\pi(w)}$, equation (5.31) becomes

$$C_{\mathcal{A}}(u) + C_{\mathcal{B}}(u) = \alpha\beta \sum \left\{ \xi^{A_i - A_{i+u}} \left[1 + (-1)^{i_{\pi(1|m)} - (i+u)_{\pi(1|m)}} \right] \left(\xi^{i_{\mathbf{1}+2x_{\pi(w)}}} + \xi^{-(i+u)_{\mathbf{1}+2x_{\pi(w)}}} \right) \right\}$$

Since $i_{\mathbf{1}+2x_{\pi(w)}} \equiv 1 + 2i_{\pi(w)}$ and $(i+u)_{\mathbf{1}+2x_{\pi(w)}} \equiv 1 + 2(i+u)_{\pi(w)}$, the third factor evaluates to

$$\xi^{1+2i_{\pi(w)}} + \xi^{-\left[1+2(i+u)_{\pi(w)}\right]} = \xi \left[(-1)^{i_{\pi(w)}} - (-1)^{-(i+u)_{\pi(w)}} \right]$$

When $i_{\pi(w)} = (i+u)_{\pi(w)}$, the factor equals zero. When $(i_{\pi(w)}, (i+u)_{\pi(w)}) = (0,1), (1,0)$, the factor equals 2ξ and -2ξ respectively. Therefore, we can again consider the three types

of terms:

Type 1: Terms in which $i_{\pi(1)} \neq (i+u)_{\pi(1)}$

Type 2: Terms in which $i_{\pi(1)} = (i+u)_{\pi(1)}$, and $i_{\pi(w)} = (i+u)_{\pi(w)}$

Type 3: Terms in which $i_{\pi(1)} = (i+u)_{\pi(1)}$, and $i_{\pi(w)} \neq (i+u)_{\pi(w)}$

Clearly, when $w = 1$, there would be no type 3 terms, as all terms would fall under the first two types.

For type 1 and type 2 terms, since the second multiplying factor and the third multiplying factor are respectively zero, the sum of these terms equal to zero.

For type 3 terms, we can use a proof similar to that used in section 5.6.2. Again, we define v to be the smallest integer for which $i_{\pi(v)} \neq j_{\pi(v)}$. By assumption, $1 < v \leq w$. Using the same invertible map to define i' and j', we can use the exact same steps in the proof detailed in section 5.6.2 to show that the constructed 16-QAM sequence is complementary. The main reason the proof still holds is because the invertible map flips the bits $i_{\pi(v-1)}$ and $(i+u)_{\pi(v-1)}$, and since $v - 1 \neq w$, $i_{\pi(w)}$ and $(i+u)_{\pi(w)}$ remain unchanged, and the term corresponding to (i', j') is also of type 3.

For the cases of $s(x_1, x_2, \cdots, x_m) = x_{\pi(w)} + 3x_{\pi(w+1)}, 2x_{\pi(w)} + 2x_{\pi(w+1)}, 3x_{\pi(w)} + x_{\pi(w+1)}, \mathbf{1} + x_{\pi(w)} + x_{\pi(w+1)}, \mathbf{1} + 3x_{\pi(w)} + 3x_{\pi(w+1)}$

We will again prove the complementarity of the constructed sequence by considering different types of terms in the sum (5.31):

$$C_{\mathcal{A}}(u) + C_{\mathcal{B}}(u) \;=\; \alpha\beta \sum_{0 \leq i, i+u \leq n-1} \left\{ \xi^{A_i - A_{i+u}} \left[1 + (-1)^{i_{\pi(1|m)} - (i+u)_{\pi(1|m)}} \right] \left(\xi^{i_s} + \xi^{-(i+u)_s} \right) \right\}$$

As the cases we consider in this subsection have many different types of summation terms, for the sake of brevity, we will present the proof for all the cases at the same time, and make use of Table 5.2 to elucidate the exposition.

We will show that the sequence $\mathcal{B}$ where $B_i = A_i + 2i_{\pi(1)}$ and $b_i = a_i + 2i_{\pi(1)}$ is complementary to sequence $\mathcal{A}$. By using a reversal of permutation argument, we can immediately obtain that the sequence $\mathcal{B}$ where $B_i = A_i + 2i_{\pi(m)}$ and $b_i = a_i + 2i_{\pi(m)}$ is also complementary to the sequences $\mathcal{A}$ described in this subsection. Note that reversing the permutation maps the case where $s(x_1, x_2, \cdots, x_m) = x_{\pi(w)} + 3x_{\pi(w+1)}$ into the case where $s(x_1, x_2, \cdots, x_m) = 3x_{\pi(w)} + x_{\pi(w+1)}$ and vice versa. This permutation reversal does not affect $s(x_1, x_2, \cdots, x_m)$ for the other three possibilities we consider in this subsection.

As before, observing that if $i_{\pi(1)} \neq (i+u)_{\pi(1)}$, the second multiplying factor in the terms of the sum above will equal to zero, and so the sum of all terms with $i_{\pi(1)} \neq (i+u)_{\pi(1)}$ is equal to zero.

Now we consider terms for which $i_{\pi(1)} = (i+u)_{\pi(1)}$. Table 5.2 below shows the value of the third factor $\xi^{i_s} + \xi^{-(i+u)_s}$ evaluated for all possible combinations of $(i_{\pi(w)}, (i+u)_{\pi(w)}, i_{\pi(w+1)}, (i+u)_{\pi(w+1)})$ for each possible expression of s considered in this subsection.

Let $j = i+u$. Define v to be the smallest integer for which $i_{\pi(v)} \neq j_{\pi(v)}$. By assumption, $v > 1$.

Case 1: $v \leq w$ or $v > w+2$

In this case, we define i' and j' using their binary representations

$$\begin{aligned} i' &= (i_1, i_2, \cdots, 1 - i_{\pi(v-1)}, \cdots, i_m) \\ j' &= (j_1, j_2, \cdots, 1 - j_{\pi(v-1)}, \cdots, j_m). \end{aligned}$$

By assumption, $i_{\pi(v-1)} = j_{\pi(v-1)}$, and so $j' = i'+u$. We have, therefore, defined an invertible map from the ordered pair (i,j) to (i',j') and since $v-1 \neq w$ or $w+1$, $i_{\pi(w)}$, $j_{\pi(w)}$, $i_{\pi(w+1)}$, $j_{\pi(w+1)}$ all remain unchanged. Therefore the terms corresponding to both pairs would have the same coefficient (coming from the third factor) in the sum. Substituting for i and i' in (5.15) gives

$$A_{i'} - A_i = 2i_{\pi(v-2)} + 2i_{\pi(v)} + c_{\pi(v-1)} - 2c_{\pi(v-1)}i_{\pi(v-1)}$$

(unless $v = 2$, in which case we just delete terms involve $\pi(v-2)$ here and in what follows). Therefore,

$$\begin{aligned} A_i - A_j - A_{i'} + A_{j'} &= 2(j_{\pi(v-2)} - i_{\pi(v-2)}) + 2(j_{\pi(v)} - i_{\pi(v)}) - 2c_{\pi(v-1)}(j_{\pi(v-1)} - i_{\pi(v-1)}) \\ &= \pm 2 \end{aligned}$$

by the definition of v. Therefore,

$$\begin{aligned} \xi^{A_i - A_j - A_{i'} + A_{j'}} &= -1 \\ \xi^{A_i - A_j} &= -\xi^{A_{i'} - A_{j'}} \\ \xi^{A_i - A_j} + \xi^{A_{i'} - A_{j'}} &= 0 \end{aligned}$$

for each pair of (i,j) and (i',j'), both of which are multiplied by the same coefficient in the sum $C_{\mathcal{A}}(u) + C_{\mathcal{B}}(u)$. Therefore, the contribution to the sum, from all terms in this case is equal to zero.

Case 2: $v = w + 1$

By the definition of v, $i_{\pi(w)} = j_{\pi(w)}$ and $i_{\pi(w+1)} \neq j_{\pi(w+1)}$. This corresponds to rows 1-2, and 5-6 in table 5.2. Note that for these pairs of rows (i.e. the pair of rows 1 and 2, and the pair of rows 5 and 6), the value of the third factor is the same.

We define i' and j' in the exact same way as the previous case. Now, even though $i_{\pi(w)}$ and $j_{\pi(w)}$ have been changed by the mapping to i' and j', we note that the mapping results in (i', j') becoming the partner combination in each pair. And from the table we can see that the value of the third factor remains unchanged. Going through the same steps as the previous case, we arrive at the conclusion that $\xi^{A_i - A_j} + \xi^{A_{i'} - A_{j'}} = 0$. Since the coefficient multiplying these two terms in the sum $C_{\mathcal{A}}(u) + C_{\mathcal{B}}(u)$ are the same, the contribution of these terms in the sum must equal to zero.

Case 3: $v = w + 2$

By the definition of v, $i_{\pi(w)} = j_{\pi(w)}$ and $i_{\pi(w+1)} = j_{\pi(w+1)}$. This corresponds to rows 11-12, and 15-16 in table 5.2. Note that for these pairs of rows (i.e. the pair of rows 11 and 12, and the pair of rows 15 and 16), the value of the third factor is the same.

Now, we define i' and j' using their binary representations

$$\begin{aligned} i' &= (i_1, i_2, \cdots, 1 - i_{\pi(w)}, \cdots, 1 - i_{\pi(w+1)}, \cdots, i_m) \\ j' &= (j_1, j_2, \cdots, 1 - j_{\pi(w)}, \cdots, 1 - j_{\pi(w+1)}, \cdots, j_m) \end{aligned}$$

Since $i_{\pi(w)} = j_{\pi(w)}$ and $i_{\pi(w+1)} = j_{\pi(w+1)}$, $j' = i' + u$. Note that this transformation maps (i, j) to (i', j') which satisfies the partner combination of $(i_{\pi(w)}, j_{\pi(w)}, i_{\pi(w+1)}, j_{\pi(w+1)})$ for the pair of rows (i, j) belongs to. This means that the value of the third factor corresponding to (i', j') is the same as that for (i, j).

Substituting for i and i' in (5.15) gives

$$A_{i'} - A_i = 2i_{\pi(w-1)} + 2 - 2i_{\pi(w)} - 2i_{\pi(w+1)} + 2i_{\pi(w+2)} + c_{\pi(w)} - 2c_{\pi(w)} i_{\pi(w)} + c_{\pi(w+1)} - 2c_{\pi(w+1)} i_{\pi(w+1)}$$

(unless $w = 1$, in which case we just delete terms that involve $\pi(w-1)$ here and in what follows).

Thus,

$$\begin{aligned} A_i - A_j - A_{i'} + A_{j'} &= 2(j_{\pi(w-1)} - i_{\pi(w-1)}) + 2(j_{\pi(w+2)} - i_{\pi(w+2)}) \\ &\quad -2(1 + c_{\pi(w)})(j_{\pi(w)} - i_{\pi(w)}) - 2(1 + c_{\pi(w+1)})(j_{\pi(w+1)} - i_{\pi(w+1)}) \\ &= \pm 2 \end{aligned}$$

$i_{\pi(w)}$	$(i+u)_{\pi(w)}$	$i_{\pi(w+1)}$	$(i+u)_{\pi(w+1)}$	$\xi^{i_s}+\xi^{-(i+u)_s}$				
				$s=x_{\pi(w)}+3x_{\pi(w+1)}$	$s=3x_{\pi(w)}+x_{\pi(w+1)}$	$s=2x_{\pi(w)}+2x_{\pi(w+1)}$	$s=\mathbf{1}+x_{\pi(w)}+x_{\pi(w+1)}$	$s=\mathbf{1}+3x_{\pi(w)}+3x_{\pi(w+1)}$
0	0	0	1	$1+\xi$	$1-\xi$	0	$-1+\xi$	$1+\xi$
1	1	0	1					
1	0	0	0				$-1-\xi$	$1-\xi$
1	0	1	1					
0	0	1	0	$1-\xi$	$1+\xi$			
1	1	1	0					
0	1	0	0				$-1+\xi$	$1+\xi$
0	1	1	1					
0	1	1	0	-2ξ	2ξ	-2	-2	2
1	0	0	1	2ξ	-2ξ			
0	0	1	1	0	0			
1	1	0	0					
0	1	0	1	2	2	2	2ξ	2ξ
1	0	1	0				-2ξ	-2ξ
0	0	0	0				0	0
1	1	1	1					

Table 5.2: Values for the third factor $\xi^{i_s}+\xi^{-(i+u)_s}$ for cases $s(x_1,x_2,\cdots,x_m)$ $=x_{\pi(w)}+3x_{\pi(w+1)}$, $2x_{\pi(w)}+2x_{\pi(w+1)}$, $3x_{\pi(w)}+x_{\pi(w+1)}$, $\mathbf{1}+x_{\pi(w)}+$ $x_{\pi(w+1)}$, $\mathbf{1}+3x_{\pi(w)}+3x_{\pi(w+1)}$

by the definition of v. Therefore,

$$\begin{aligned} \xi^{A_i - A_j - A_{i'} + A_{j'}} &= -1 \\ \xi^{A_i - A_j} &= -\xi^{A_{i'} - A_{j'}} \\ \xi^{A_i - A_j} + \xi^{A_{i'} - A_{j'}} &= 0 \end{aligned}$$

for each pair of (i, j) and (i', j'), both of which are multiplied by the same coefficient in the sum $C_{\mathcal{A}}(u) + C_{\mathcal{B}}(u)$. Therefore, the contribution to the sum, from all terms in this case, is equal to zero.

Since the contribution of all the various types of terms is zero, the sum $C_{\mathcal{A}}(u) + C_{\mathcal{B}}(u)$ must equal zero, for $u \neq 0$. Therefore $\mathcal{A}$ and $\mathcal{B}$ are complementary 16-QAM sequences.

Adding 2 to $s(x_1, x_2, \cdots, x_m)$ in the above cases

Adding **2** to $s(x_1, x_2, \cdots, x_m)$ in the above cases simply negates the third factor since

$$\begin{aligned} \xi^{i_{\mathbf{2}+s}} + \xi^{-(i+u)_{\mathbf{2}+s}} &= \xi^{2+i_s} + \xi^{-2-(i+u)_s} \\ &= -\xi^{i_s} - \xi^{-(i+u)_s} = -\left[\xi^{i_s} + \xi^{-(i+u)_s}\right]. \end{aligned}$$

As no part of the proof in all the previous subsections relies on the actual value of the third factor when it is non-zero, negating the factor consistently throughout the proof will not change the conclusion that we arrive at, namely, that the sum of all the terms in $C_{\mathcal{A}}(u) + C_{\mathcal{B}}(u)$ is equal to zero.

Therefore, we can safely add **2** to $s(x_1, x_2, \cdots, x_m)$ in all the above cases and double the number of 16-QAM sequences we have constructed and proven to be complementary.

5.6.3 PMEPR Bounds for Constructed Complementary 16-QAM Sequences

Consider the rectangular 16-QAM signal constellation where adjacent symbols are equidistant from one another. Assuming the 16-QAM signal constellation has been normalized to have unit energy, we can see from the above figure that adding 0 to the major coordinate results in a 16-QAM symbol with energy 1.8, adding 1 or 3 results in a 16-QAM symbol with energy 1.0, and adding 2 results in a 16-QAM symbol with energy 0.2.

Thus the energy of any constructed 16-QAM sequence can be calculated by counting the number of 0's, 1's, 2's and 3's in the sequence that is added elementwise to the major coordinate sequence. And since we have shown that the complementary pairs to the constructed

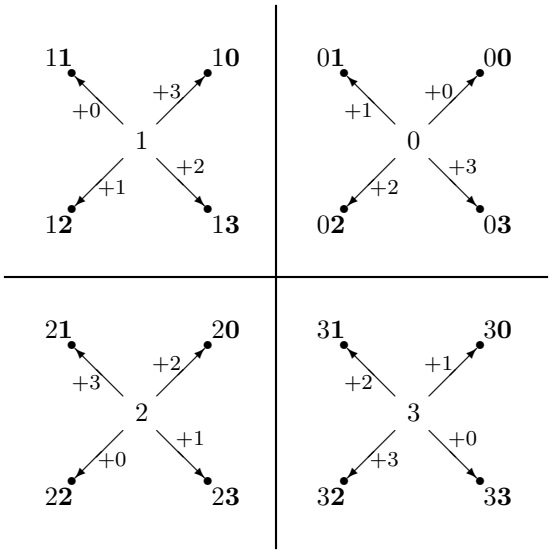

Figure 5-5: Graphical representation of construction of 16-QAM symbols from two 4-QAM symbols

sequences are sequences with $B_i = A_i + 2i_{\pi(1|m)}$, $b_i = a_i + 2i_{\pi(1|m)}$, these complementary pairs of sequences have the same power because each element in the complementary pair is either the same as the 16-QAM symbol in the original sequence (when $i_{\pi(1|m)} = 0$) or the negative of the 16-QAM symbol (when $i_{\pi(1|m)} = 1$). Lemma 5.6 tells us that the mean envelope power (averaging over all the constructed sequences) is n. Thus the PMEPR bound for $\mathcal{A}$ is equal to $\frac{1}{n}\left(P_{\mathcal{A}} + P_{\mathcal{B}}\right) = \frac{2}{n}P_{\mathcal{A}}$. Table 5.3 list the PMEPR bounds for each case in our construction of complementary 16-QAM sequences, and table 5.4 summarizes the number of constructed sequences for each of the five different PMEPR bounds.

Our construction gives us complementary 16-QAM sequences with easily calculated PMEPR bounds. We have not only defined a much larger set of codes than described in [5] and [6], we have also calculated tighter PMEPR bounds for the codes.

5.6.4 Code Rates for Constructed Complementary 16-QAM Sequences

Table 5.5 shows the code rates of the constructed complementary 16-QAM sequences for various values of sequence length $n = 2^m$.

We can see that for small n, using the constructed sequences give a reasonable code rate, but the rate drops pretty quickly as the length of sequence increases. Thus, the constructed

$s(x_1, x_2, \cdots, x_m)$	Number of Possibilities	Number of 0's	Number of 1's	Number of 2's	Number of 3's	PMEPR Bound
$\mathbf{0}$	1	n	0	0	0	3.6
$x_{\pi(1)}$	1	$n/2$	$n/2$	0	0	2.8
$x_{\pi(m)}$	1	$n/2$	$n/2$	0	0	2.8
$2x_{\pi(1)}$	1	$n/2$	0	$n/2$	0	2.0
$2x_{\pi(m)}$	1	$n/2$	0	$n/2$	0	2.0
$3x_{\pi(1)}$	1	$n/2$	0	0	$n/2$	2.8
$3x_{\pi(m)}$	1	$n/2$	0	0	$n/2$	2.8
$x_{\pi(w)} + 3x_{\pi(w+1)}$	$m-1$	$n/2$	$n/4$	0	$n/4$	2.8
$2x_{\pi(w)} + 2x_{\pi(w+1)}$	$m-1$	$n/2$	0	$n/2$	0	2.0
$3x_{\pi(w)} + x_{\pi(w+1)}$	$m-1$	$n/2$	$n/4$	0	$n/4$	2.8
$\mathbf{1}$	1	0	n	0	0	2.0
$\mathbf{1} + x_{\pi(1)}$	1	0	$n/2$	$n/2$	0	1.2
$\mathbf{1} + x_{\pi(m)}$	1	0	$n/2$	$n/2$	0	1.2
$\mathbf{1} + 3x_{\pi(1)}$	1	$n/2$	$n/2$	0	0	2.8
$\mathbf{1} + 3x_{\pi(m)}$	1	$n/2$	$n/2$	0	0	2.8
$\mathbf{1} + 2x_{\pi(w)}$	m	0	$n/2$	0	$n/2$	2.0
$\mathbf{1} + x_{\pi(w)} + x_{\pi(w+1)}$	$m-1$	0	$n/4$	$n/2$	$n/4$	1.2
$\mathbf{1} + 3x_{\pi(w)} + 3x_{\pi(w+1)}$	$m-1$	$n/2$	$n/4$	0	$n/4$	2.8
$\mathbf{2}$	1	0	0	n	0	0.4
$\mathbf{2} + x_{\pi(1)}$	1	0	0	$n/2$	$n/2$	1.2
$\mathbf{2} + x_{\pi(m)}$	1	0	0	$n/2$	$n/2$	1.2
$\mathbf{2} + 2x_{\pi(1)}$	1	$n/2$	0	$n/2$	0	2.0
$\mathbf{2} + 2x_{\pi(m)}$	1	$n/2$	0	$n/2$	0	2.0
$\mathbf{2} + 3x_{\pi(1)}$	1	0	$n/2$	$n/2$	0	1.2
$\mathbf{2} + 3x_{\pi(m)}$	1	0	$n/2$	$n/2$	0	1.2
$\mathbf{2} + x_{\pi(w)} + 3x_{\pi(w+1)}$	$m-1$	0	$n/4$	$n/2$	$n/4$	1.2
$\mathbf{2} + 2x_{\pi(w)} + 2x_{\pi(w+1)}$	$m-1$	$n/2$	0	$n/2$	0	2.0
$\mathbf{2} + 3x_{\pi(w)} + x_{\pi(w+1)}$	$m-1$	0	$n/4$	$n/2$	$n/4$	1.2
$\mathbf{3}$	1	0	0	0	n	2.0
$\mathbf{3} + x_{\pi(1)}$	1	$n/2$	0	0	$n/2$	2.8
$\mathbf{3} + x_{\pi(m)}$	1	$n/2$	0	0	$n/2$	2.8
$\mathbf{3} + 3x_{\pi(1)}$	1	0	0	$n/2$	$n/2$	1.2
$\mathbf{3} + 3x_{\pi(m)}$	1	0	0	$n/2$	$n/2$	1.2
$\mathbf{3} + 2x_{\pi(w)}$	m	0	$n/2$	0	$n/2$	2.0
$\mathbf{3} + x_{\pi(w)} + x_{\pi(w+1)}$	$m-1$	$n/2$	$n/4$	0	$n/4$	2.8
$\mathbf{3} + 3x_{\pi(w)} + 3x_{\pi(w+1)}$	$m-1$	0	$n/4$	$n/2$	$n/4$	1.2

Table 5.3: PMEPR bounds for constructed 16-QAM sequences

PMEPR Bound	No. of Possibilities per Major Sequence	Total No. of Constructed Sequences
3.6	1	$\frac{m!}{2}4^{m+1}$
2.8	$4+4m$	$(4+4m)\frac{m!}{2}4^{m+1}$
2.0	$4+4m$	$(4+4m)\frac{m!}{2}4^{m+1}$
1.2	$4+4m$	$(4+4m)\frac{m!}{2}4^{m+1}$
0.4	1	$\frac{m!}{2}4^{m+1}$

Table 5.4: No. of constructed 16-QAM sequences grouped according to PMEPR bound

Sequence Length	$\log_2$(No. of Constructed Sequences)	Code Rate
4	11.2479	0.7030
8	15.2288	0.4759
16	19.5392	0.3053
32	24.1163	0.1884
64	28.9181	0.1130
128	33.9139	0.0662
256	39.0806	0.0382
512	44.3999	0.0217
1024	49.8572	0.0122

Table 5.5: Code rates of constructed 16-QAM sequences

sequences would not be suitable for general use as codes for OFDM systems with a large number of subcarriers (> 32). However, the constructed sequences could still see practical application in the design of pilot symbols, as well as in scenarios where peak power control and encoder complexity are overriding concerns, not code rate. One such scenario could be in mobile handsets, where high peaks in the transmitted signal would have a deleterious effect on battery life.

5.7 8-QAM Complementary Sequences

Consider the construction of 16-QAM complementary sequences from two 4-QAM sequences described in section 5.6. Suppose now that we limit the possible values for the major

coordinates A_i to be either 0 or 2. Thus the general form for $a_{\text{major}}(x_1, x_2, \cdots, x_m)$ is

$$a_{\text{major}}(x_1, x_2, \cdots, x_m) = 2\sum_{k=1}^{m-1} x_{\pi(k)}x_{\pi(k+1)} + 2\sum_{k=1}^{m} c_k x_k + 2 \cdot \mathbf{c}$$

where $c_k \in \{0, 1\}$ and $\mathbf{c} = \mathbf{0}$ or $\mathbf{1}$.

Using the same $14 + 12m$ possible monomials as listed in section 5.6 to obtain the minor coordinates, and setting α to $\frac{1}{\sqrt{5}}$ and β to $\frac{2}{\sqrt{5}}$ (chosen to normalize the constellation to have unit average energy), we obtain sequences of symbols coming from the 8-QAM constellation pictured in figure 5-6.

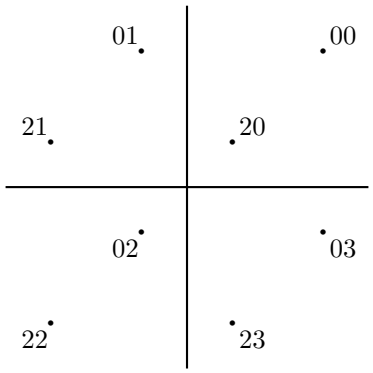

Figure 5-6: 8-QAM Signal Constellation

Since this is only a special case of the construction described in section 5.6, the proof of complementarity for the constructed sequences still holds, and we have thus demonstrated a construction of 8-QAM complementary sequences. This construction results in a total of $(14 + 12m)(m!/2)2^{m+1}$ complementary sequences with two sets of $(m!/2)2^{m+1}$ sequences each having PMEPR bounds of 3.6 and 0.4 respectively, and three sets of $(4 + 4m)(m!/2)2^{m+1}$ sequences each having PMEPR bounds of 2.8, 2.0, and 1.2 respectively.

Chapter 6

Conclusion

6.1 Summary

In this thesis, we began by explaining the fundamentals of Orthogonal Frequency Division Multiplexing (OFDM). We then focussed on one particular problem of OFDM, that of high peak-to-mean envelope power ratios (PMEPRs). We discussed several possible solutions, other than the main approach taken in this thesis, which is that of using codes which yield signals with low PMEPRs.

Starting with Golay complementary sequences, we showed that when applied as codes in OFDM system, they provide signals with low PMEPRs. Building on the results of Davis and Jedwab [1] which link Golay complementary sequences to Reed-Muller codes, we constructed new codes using symbols in 4-QAM and 16-QAM constellations with low PMEPR and encoding complexity. Moreover, the 16-QAM sequences constructed were also proven to be complementary. Although the 4-QAM codes we construct are not, in general, complementary, they are amenable to relatively simple decoding algorithms. As a special case of the 16-QAM sequence construction, we obtained 8-QAM complementary sequences in a straightforward manner.

6.2 Future Research Possibilities

Two areas for further research arise immediately from the research work presented here. The first is in providing efficient decoding algorithms for the 16-QAM complementary sequences constructed in section 5.6, and the second is in finding code structures for other signal

constellations, such as 32-QAM and 64-QAM.

The 8-QAM complementary sequence construction proposed in section 5.7 gives us $(14+12m)\frac{m!}{2}2^{m+1}$ sequences which are easily encodable. However, this number is relatively small, and it appears that we might be able to do better with an alternative coding scheme.

Having shown the possibility of constructing complementary sequences in higher-order constellations from those of lower-order constellations, it would be interesting to pursue the same line of reasoning for 32-QAM (16-QAM + BPSK, or 8-QAM + 4-QAM?), 64-QAM (4-QAM + 4-QAM + 4-QAM?), and higher order constellations.

Bibliography

[1] James A. Davis and Jonathan Jedwab. Peak-to-mean power control in OFDM, Golay complementary sequences, and Reed-Muller codes. *IEEE Transactions on Information Theory*, 45(7):2397–2417, November 1999.

[2] Robert L. Frank. Polyphase complementary codes. *IEEE Transactions on Information Theory*, IT-26:641–647, November 1980.

[3] Marcel J. E. Golay. Complementary series. *IRE Transactions on Information Theory*, IT-7:82–87, April 1961.

[4] Kenneth G. Paterson. Generalized Reed-Muller codes and power control in OFDM modulation. *IEEE Transactions on Information Theory*, 46(1):104–120, January 2000.

[5] Cornelia Rößing. Golay complementary sequences for OFDM with 16-QAM. *IEEE Proceedings of International Symposium on Information Theory*, page 331, June 2000.

[6] Cornelia Rößing and Vahid Tarokh. A construction of OFDM 16-QAM sequences having low peak powers. To be published.

[7] R. Sivaswamy. Multiphase complementary codes. *IEEE Transactions on Information Theory*, pages 546–552, 1978.

[8] Rüdiger Urbanke and A. S. Krishnakumar. Compact description of golay sequences and their extensions. *Proceedings 34th Annual Allerton Conference on Communication, Control, and Computing*, pages 693–702, October 1996.

[9] Richard Van Nee and Ramjee Prasad. *OFDM for Wireless Multimedia Communications*. Artech House Publishers, Boston, MA, 2000.